Circulation Research
JOURNAL OF THE AMERICAN HEART ASSOCIATION

Genome Editing of Human Embryonic Stem Cells and Induced Pluripotent Stem Cells With Zinc Finger Nucleases for Cellular ImagingNovelty and Significance

Yongming Wang, Wendy Y. Zhang, Shijun Hu, Feng Lan, Andrew S. Lee, Bruno Huber, Leszek Lisowski, Ping Liang, Mei Huang, Patricia E. de Almeida, Jong H. Won, Ning Sun, Robert C. Robbins, Mark A. Kay, Fyodor D. Urnov and Joseph C. Wu

Circ Res. 2012;111:1494-1503; originally published online September 11, 2012;
doi: 10.1161/CIRCRESAHA.112.274969
Circulation Research is published by the American Heart Association, 7272 Greenville Avenue, Dallas, TX 75231

Print ISSN: 0009-7330. Online ISSN: 1524-4571

Genome Editing of Human Embryonic Stem Cells and Induced Pluripotent Stem Cells With Zinc Finger Nucleases for Cellular Imaging

Yongming Wang,* Wendy Y. Zhang,* Shijun Hu, Feng Lan, Andrew S. Lee, Bruno Huber, Leszek Lisowski, Ping Liang, Mei Huang, Patricia E. de Almeida, Jong H. Won, Ning Sun, Robert C. Robbins, Mark A. Kay, Fyodor D. Urnov, Joseph C. Wu

Rationale: **Molecular imaging has proven to be a vital tool in the characterization of stem cell behavior in vivo. However, the integration of reporter genes has typically relied on random integration, a method that is associated with unwanted insertional mutagenesis and positional effects on transgene expression.**

Objective: **To address this barrier, we used genome editing with zinc finger nuclease (ZFN) technology to integrate reporter genes into a safe harbor gene locus (PPP1R12C, also known as AAVS1) in the genome of human embryonic stem cells and human induced pluripotent stem cells for molecular imaging.**

Methods and Results: **We used ZFN technology to integrate a construct containing monomeric red fluorescent protein, firefly luciferase, and herpes simplex virus thymidine kinase reporter genes driven by a constitutive ubiquitin promoter into a safe harbor locus for fluorescence imaging, bioluminescence imaging, and positron emission tomography imaging, respectively. High efficiency of ZFN-mediated targeted integration was achieved in both human embryonic stem cells and induced pluripotent stem cells. ZFN-edited cells maintained both pluripotency and long-term reporter gene expression. Functionally, we successfully tracked the survival of ZFN-edited human embryonic stem cells and their differentiated cardiomyocytes and endothelial cells in murine models, demonstrating the use of ZFN-edited cells for preclinical studies in regenerative medicine.**

Conclusions: **Our study demonstrates a novel application of ZFN technology to the targeted genetic engineering of human pluripotent stem cells and their progeny for molecular imaging in vitro and in vivo. (*Circ Res*. 2012;111:1494-1503.)**

Key Words: homologous recombination ■ induced pluripotent stem cells ■ molecular imaging ■ reporter gene ■ zinc finger nuclease

Both human embryonic stem cells (hESCs) and induced pluripotent stem cells (iPSCs) hold great promise in the field of regenerative medicine.[1–5] These cells are characterized by their indefinite self-renewing ability and pluripotent differentiation potential. Because these cells possess the ability to differentiate into all somatic cell types present in the human body,[6] in theory hESCs and iPSCs are ideal therapeutic donor sources, as exemplified by the recent first-in-human trial involving the transplantation of hESC-differentiated retinal pigment epithelium (RPE) in patients with dry age-related macular degeneration and Stargardt's macular dystrophy.[7] However, further research has brought to light many issues regarding the direct delivery of these stem cells and their derivatives. Cell survival, teratoma formation, host immune rejection, and cellular migration outside the area of administration are among the most pressing challenges.[8–10] Thus, investigation into the in vivo behavior of transplanted cells is essential for both the full understanding of stem cells' therapeutic potential and their subsequent clinical applications.

Editorial, see p 1486

Molecular imaging has offered researchers an accurate, non-invasive, and sensitive means to longitudinally track in vivo cell behavior.[10–14] It has proven to be the most effective tracking modality for the study of cell survival and proliferation over time. In fact, reporter gene–based molecular imaging has been used

Original received June 2, 2012; revision received August 29, 2012; accepted September 11, 2012. In July 2012, the average time from submission to first decision for all original research papers submitted to *Circulation Research* was 11.48 days.

From the Department of Medicine, Division of Cardiology (Y.W., W.Y.Z., S.H., F.L., A.S.L., B.H., P.L., M.H., P.E.d.A., J.H.W., N.S., J.C.W.), Department of Radiology, Molecular Imaging Program (Y.W., W.Y.Z., S.H., F.L., A.S.L., B.H., P.L., M.H., P.E.d.A., J.H.W., N.S., J.C.W.), Institute for Stem Cell Biology and Regenerative Medicine (A.S.L., J.C.W.), Departments of Pediatrics and Genetics (L.L., M.A.K.), and Cardiovascular Institute (R.C.R., J.C.W.), Stanford School of Medicine, Stanford, CA; and Sangamo Biosciences, Richmond, CA (F.D.U.).

*These authors contributed equally to this work.

The online-only Data Supplement is available with this article at http://circres.ahajournals.org/lookup/suppl/doi:10.1161/CIRCRESAHA.112.274969/-/DC1.

Correspondence to Joseph C. Wu, Lorry Lokey Stem Cell Research Bldg, 265 Campus Dr, Room G1120B, Stanford, CA 94305-5111. E-mail joewu@stanford.edu

Non-standard Abbreviations and Acronyms	
aMHC	a-myosin heavy chain
BLI	bioluminescence imaging
CM	cardiomyocyte
EB	embryoid body
EC	endothelial cell
FLI	fluorescence imaging
hESC	human embryonic stem cell
Fluc	firefly luciferase
HSVtk	herpes simplex virus thymidine kinase
iPSC	induced pluripotent stem cell
MI	myocardial infarction
mRFP	monomeric red fluorescent protein
PCR	polymerase chain reaction
PET	positron emission tomography
PPP1R12C	protein phosphatase 1, regulatory subunit 12C
ZFN	zinc finger nuclease

to track teratoma formation, cell survival, and host immune rejection for both hESCs and iPSCs.[8–10,15] However, clinical translatability of modified cells for reporter gene–based imaging has been hampered by current transgenesis methods using random integration,[16,17] which is suboptimal for the following reasons: (1) The cell lines resulting from this method are nonisogenic, with some cells bearing single copies of the reporter gene, whereas others bearing multiple copies; (2) if the reporter genes are inserted into a closed locus or if 1 cell contains multiple copies, expression driven by the reporter genes tends to be unstable over time as a result of epigenetic effects[18,19]; and (3) it has been observed that insertional mutagenesis resulting from random integration can be severely detrimental to the biology of the stem cells.[20,21] Imaging heterogeneous populations of these cells could lead to inaccurate assessment of in vivo cell behavior. Furthermore, from a clinical translation and regulatory perspective, batches of hESCs or iPSCs carrying a transgene at multiple random locations pose difficulties because the final product is biologically nonhomogeneous.

An added challenge in this regard comes from the use of transgenic hESCs and iPSCs for animal disease models as well as disease in a dish efforts. The development of iPSC technology has fostered great interest in understanding the impact that interpersonal genome variation has on phenotypic differences, and, consequently, large numbers of iPSC lines are being generated for that purpose. To allow a comparison of the iPSC in vitro and in vivo properties, reporter genes are indispensable, but it is essential to avoid the insertional effects of the reporter and the confounding effects of multiple reporter gene copies. Therefore, a safe targeted transgenesis method supporting long-term gene expression is vital to the translatability of molecular imaging for in vivo cell tracking. In the present work, we set out to develop a method to comprehensively solve this problem by using human genome editing.[22] This technology relies on an engineered zinc finger nuclease (ZFN) to induce a double-strand break,[23] which then allows targeted gene repair,[24] knockout,[25] or transgene integration.[26] Earlier work has established genome editing in hESCs and iPSCs.[27] Here, we wanted to investigate whether the ZFNs we developed for targeted gene addition to a genomic safe harbor[22] could be used to track the fate of hESCs and iPSCs in vitro and in vivo.

Classical work from the Soriano laboratory on the Rosa26 locus[28] prompted a complementary effort in human cells. The PPP1R12C gene on chromosome 19, also known as AAVS1, can be used as a landing pad for ZFN-directed transgenes to allow for their long-term expression.[22] AAVS1 is dispensable in hESCs and iPSCs when knocked out with either ZFNs[22,29] or TAL effector nucleases (TALENs).[30] or made hemizygous by conventional gene targeting,[31] and also can carry transgenes in such a way that transcription of neighboring genes is not affected.[32] We reasoned that we could rely on genome editing to establish a method to rapidly generate isogenic hESC and iPSC panels carrying distinct reporters at the same genomic location.

The key aim of this study was to establish a platform for in vivo imaging of hESCs and iPSCs and their differentiated progeny. For this purpose, we introduced a reporter construct containing mRFP for FLI firefly luciferase (Fluc) for bioluminescence imaging (BLI), and herpes simplex virus thymidine kinase (HSVtk) for positron emission tomography (PET) imaging into the AAVS1 locus using ZFN-driven genome editing. Our results demonstrate that such ZFN-edited stem cells maintain long-term and robust reporter gene expression and can be accurately monitored by both BLI and PET imaging in live animals. Our data establish a turnkey method for rapidly generating isogenic hESCs and iPSCs carrying any number of reporter constructs for both in vitro and in vivo cell fate tracking.

Methods

Cell Culture and Maintenance of Human Pluripotent Stem Cells

For derivation of human iPSC line, see the Online Methods. Human ESCs (WA09; Wicell, Madison, WI) and iPSCs were cultured on Matrigel-coated plates (ES qualified; BD Biosciences, San Diego, CA) using mTeSR-1 cell culture medium (StemCell Technologies, Vancouver, Canada) under conditions of 37°C, 95% air, and 5% CO_2 in a humidified incubator, as previously described.[33] Cells were passaged via dissociation with collagenase IV (Invitrogen) every 4 to 6 days.

Construction of an AAVS1-TF Donor Plasmid for ZFN-Mediated Integration

The DNA fragment containing monomeric red fluorescent protein-Fluc-HSVtk reporter genes was polymerase chain reaction (PCR)–amplified from the triple fusion (TF) construct (pFU-UFRTW)[34] with primers GGGGGGACATGTCAGCAGAGATCCA GTTTGGTT/GGGGCGCGCCCCACATAGCGTAAAAGGAGCA and digested with restriction enzymes PciI and AscI (New England BioLabs). The fragment was then inserted into the MluI/NcoI cut site of the donor plasmid AAVS1-CAGGS–enhanced green fluorescent protein (eGFP) backbone (Addgene, Cambridge, MA).[22] The resultant donor plasmid, p5_AAVS1-SA-puro-pA-CAG- mRFP-Fluc-HSVtk-pA-3_AAVS1 (referred to hereafter as AAVS1-TF), contains a splice acceptor element and a 2A linker placed in front of a promoterless puromycin-polyA cassette, which expresses the puromycin resistance element only if inserted downstream of a constitutively active promoter, such as the PPP1R12C promoter. The triple-fusion minigene cassette driven by the human ubiquitin promoter was placed downstream of the puromycin resistance element.

Targeted Gene Addition Using AAVS1 ZFNs

In brief, 2×10^5 hESCs or iPSCs were dissociated for 3 to 4 minutes using Accutase (Sigma) and neutralized by mTeSR-1 cell culture medium. The cells were centrifuged at 100*g* for 5 minutes, washed with PBS, and resuspended in R buffer (Neon Transfection system; Invitrogen) with a total of 4 μg of AAVS1-TF donor plasmids and 500 ng of the AAVS1 ZFN-encoding plasmids.[22] The cells were transfected with the Neon Transfection system (Invitrogen) at 1100 V, 20 ms, and 1 pulse. Cells were then immediately plated onto Matrigel-coated plates with 10 μmol/L ROCK inhibitor Y27632 (Stemgent). Puromycin selection (0.2 μg/mL) was started at day 5. After a week of selection, individual clones were picked and expanded in puromycin-free culture. In addition to the single cell–derived clones, we derived several cell pools (H7, JL, 16W, and FB) transgenic for a ZFN-directed transgene cassette at AAVS1.

Genomic PCR to Detect Reporter Gene Addition

Refer to the Online Methods for more details.

Southern Blot of ZFN-Mediated HR-Targeted hESCs and iPSCs

Genomic DNA was digested with XmnI and BglII, separated on a 0.7% agarose gel, transferred to a nylon membrane (Amersham), and hybridized with ^{32}P-labeled random primer (Stratagene) probes.

Embryoid Body Formation

Refer to the Online Methods for more details.

Pluripotency Markers and Embryoid Body Analysis

Refer to the Online Methods for more details.

BLI for Longitudinal Tracking of Cell Fate

Refer to the Online Methods for more details.

PET Imaging for Longitudinal Tracking of Cell Fate

Refer to the Online Methods for more details.

Differentiation of Pluripotent Stem Cell–Derived Cardiomyocytes

Cardiomyocyte (CM) differentiation was performed following a protocol described by Laflamme et al,[35] with minimal modification. In brief, 2×10^6 undifferentiated ESCs were detached by Accutase (Sigma) and seeded onto Matrigel-coated plates (ES qualified; BD Biosciences, San Diego, CA) using mTeSR-1 cell culture medium for 1 day. To induce cardiac differentiation, we replaced mTeSR-1 medium with RPMI-B27 medium (Invitrogen), supplemented with the following cytokines: 100 ng/mL human recombinant activin A (R&D Systems) for 24 hours, followed by 10 ng/mL human recombinant Bone morphogenetic protein 4 (BMP4, R&D Systems) for 4 days. The medium was then exchanged for RPMI-B27 without supplementary cytokines; cultures were refed every 2 days for 13 additional days. Widespread spontaneous beating activity was typically observed by day 14 after addition of activin A. After 18 days of in vitro differentiation, cells were enzymatically dispersed for implantation using blendzyme IV (prepared at 0.56 U/mL in PBS; Roche) and DNAse (60 U/mL; Invitrogen) for 30 minutes at 37°C and enriched for CMs by separation over a discontinuous Percoll gradient.

Differentiation of Pluripotent Stem Cell–Derived Endothelial Cells

To derive ZFN-edited or unedited endothelial cells (ECs), we performed the differentiation protocol described by Li et al.[36] Briefly, we cultured undifferentiated hESCs in differentiation medium on Ultra-low attachment plates (Corning Incorporated, Corning, NY) for embryoid body (EB) formation. Differentiation medium consisted of Iscove's modified Dulbecco's medium with 16 BSA, insulin, transferrin (StemCell Technologies), 15% knockout TM serum replacement (Invitrogen, Carlsbad, CA), 2 mmol/L L-glutamine, 450 mmol/L monothioglycerol (Sigma, St. Louis, MO), 20 ng/mL basic fibroblast growth factor (bFGF), 0.1 mmol/L nonessential amino acids, 50 ng/mL vascular endothelial growth factor (R&D Systems Inc), 50 mg/mL streptomycin, and 50 U/mL penicillin supplemented. Twelve days after differentiation, EBs were collected and resuspended in 1.5 mg/mL rat tail collagen type I (Becton Dickinson, San Jose, CA), then plated onto 6-well plates and incubated for 30 minutes at 37°C. On gel formation, each dish received an addition of EGM-2 medium (Lonza, Basel, Switzerland) with 5% knockout TM serum replacement, 50 ng/mL vascular endothelial growth factor, and 20 ng/mL bFGF and was then further incubated for 3 days without media change.

Results

Rapid and Efficient ZFN-Mediated Targeted Reporter Addition Into the AAVS1 Safe Harbor Locus in hESCs

To overcome the limitations inherent in random integration of reporter genes, we designed a series of experiments to use ZFN technology for engineering human pluripotent stem cells for molecular imaging (Figure 1A). We designed a multifunctional reporter construct flanked by short (800 bp) stretches of homology to the ZFN target site[22] on chromosome 19 in exon 1 of the PPP1r12C gene (Figure 1B). A useful feature of this site is that it lies downstream of exon 1 of a transcribed gene[22]; we therefore included a promotorless selectable marker in our donor construct to maximize efficiency of isolating the desired cell.[22] The reporter cassette, driven by the ubiquitin promoter, is a TF gene of mRFP, Fluc, and HSVtk supporting FLI, BLI, and PET imaging, respectively.[34] We introduced the reporter construct and the ZFN expression vector into hESCs (H9) by electroporation; after puromycin selection, 6 clones were screened by genomic PCR, all of which carried the transgenic cassette at the ZFN-specified location (Figure 1C). Bona fide–targeted addition was confirmed by Southern blotting on 4 single cell–derived clones (designated as ZT1-4). As shown in Figure 1D, clones ZT2 and ZT3 carried the reporter cassette integrated on both copies of the AAVS1 locus, and clones ZT1 and ZT4 on 1 copy. Clone ZT1 also contained an additional randomly integrated reporter transgene. We also tested for the potential random integration of the ZFN expression plasmid with Southern blotting. The data revealed that there is no random integration of ZFN expression plasmid DNA in these edited cells (Online Figure IA). We next genotyped a panel of putative ZFN off-target sites in clones ZT2-4 (Online Figure IB and IC) and the unedited allele of the AAVS1 in clone ZT4 (Online Figure ID and IE); our data demonstrate all to be wild type, in agreement with previous studies on the robust specificity of this ZFN set.[22,29] In addition to the H9 line, we edited another hESC line, H7, using the same constructs. Successful integration of the reporter gene was confirmed by PCR (Online Figure IF).

ZFN-Mediated Targeting of Human iPSCs

Next, we tested the ZFN integration system in iPSCs. To derive clinically translatable iPSCs, we generated several nonviral, transgene-free iPSCs using nonintegrating, episomal minicircle DNA vectors created in our laboratory.[37] The resulting iPSC lines expressed high levels of pluripotency markers and spontaneously formed 3 germ layers both in vitro

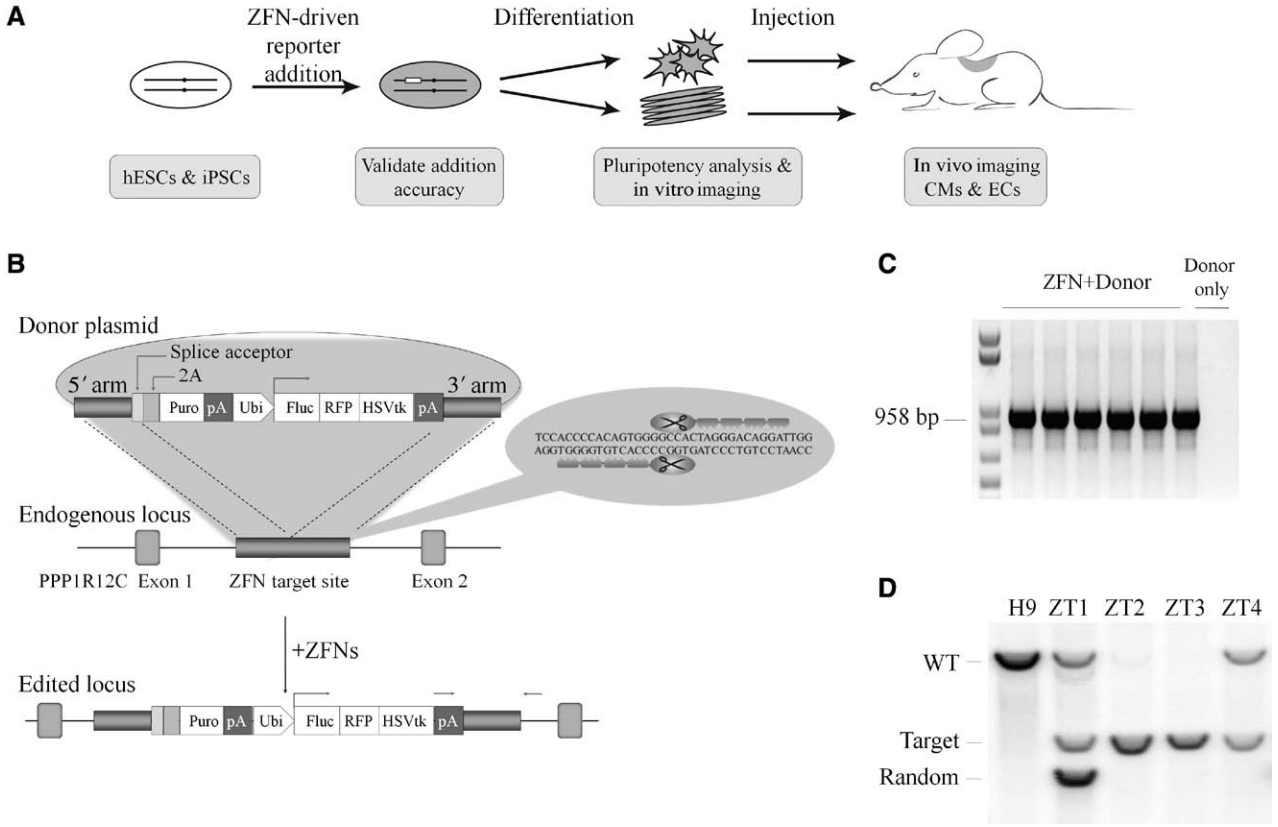

Figure 1. Zinc finger nuclease (ZFN)–driven reporter gene addition to the AAVS1 locus. A, Schematic diagram of the experiment design. First, reporter genes are integrated into AAVS1 locus using ZFN technology, and the specificity of the addition process is validated. Second, the pluripotency of ZFN-edited pluripotent stem cells (PSCs) is investigated. Third, the molecular imaging ability of ZFN-edited cells is tested both in vitro and in vivo. Finally, an application example of PSC-derived cardiomyocytes (CMs) and endothelial cells (ECs) is demonstrated. **B**, Schematic diagram of donor plasmid and endogenous AAVS1 locus after reporter gene addition. The donor plasmid contains a triple fusion reporter gene and a puromycin selection marker between 2 arms homologous to the targeting site, which is located in the first intron of PPP1R12C gene. ZFNs generate a double-strand break at the targeting site, which promotes homologous recombination. Reporter genes can insert into the AAVS1 locus by homologous recombination. Green boxes: the first 2 exons of PPP1R12C gene; pink box: the 2A ribosome stuttering signal; gray box: polyadenylation signal (pA); red arrow: primers used to detect targeted integration. Puro indicates puromycin resistance gene; Ubi, ubiquitin promoter; **C**, Detection of reporter gene addition by genomic polymerase chain reaction (PCR). All 6 clones screened are PCR positive, whereas the control cells that were only transfected with reporter construct (without ZFN expression constructs) are PCR negative. **D**, Southern blot analysis of gene addition shows that ZT1 and ZT4 clones contain single-copy–targeted integrations, whereas ZT2 and ZT3 clones contain targeted integrations into both AAVS1 sites. Clone ZT1 also contains a random integration. hESC indicates human embryonic stem cells; iPSC, induced pluripotent stem cells; Fluc, firefly luciferase; RFP, red fluorescent protein; HSVtk, herpes simplex virus thymidine kinase; and WT, wild type.

with EB formation and in vivo when injected into murine recipients (Online Figure IIA–IIC). ZFN-driven targeted reporter addition to the AAVS1 locus was comparably efficient in the iPSCs (Online Figure IID). We also edited 3 more iPSC lines generated in our laboratory with the TF construct and an iPSC line with cardiac-specific promoter myosin heavy chain driving eGFP reporter construct (Online Figure IIE). The reporter gene addition was confirmed by PCR (Online Figure IIF).

Preservation of Cell Pluripotency After ZFN Editing

To determine whether the genetic engineering and subsequent drug selection would affect stemness, we tested the pluripotency of our cells after ZFN editing and observed that all 3 ZFN-edited cell lines displayed normal morphology relative to control unedited H9 cells (Online Figure III). Further testing revealed that ZFN-edited cells maintained their pluripotent state, as indicated by the expression of pluripotency markers Oct4, Tra-1–60, Sox2, Tra-1–81, Nanog, and SSEA4 (Figure 2A). Functionally, these cells were capable of differentiation into all 3 germ layers both in vivo (Figure 2B) and in vitro (Figure 2C). We also observed spontaneous EB beating after 2 weeks of differentiation (Online Video I). All ZFN-edited cells exhibited normal karyotypes (Figure 2D). Analysis of ZFN-edited iPSCs was also performed. These cells similarly maintained pluripotency, as demonstrated by pluripotency marker expression and EB formation (Online Figure IVA and IVB). In conclusion, both hESCs and iPSCs maintained their pluripotent potential after ZFN-mediated addition of reporter genes to the AAVS1 locus and subsequent drug selection.

In Vitro Imaging of ZFN-Edited Cells

To verify the functionality of the reporter genes in the ZFN-edited stem cells, we tested the edited hESCs for expression of the integrated Fluc and HSVtk reporter genes. All 3 ZFN-edited cell lines showed robust BLI and PET signals (Figure 3A and 3B). Importantly, when ZFN-edited hESCs were

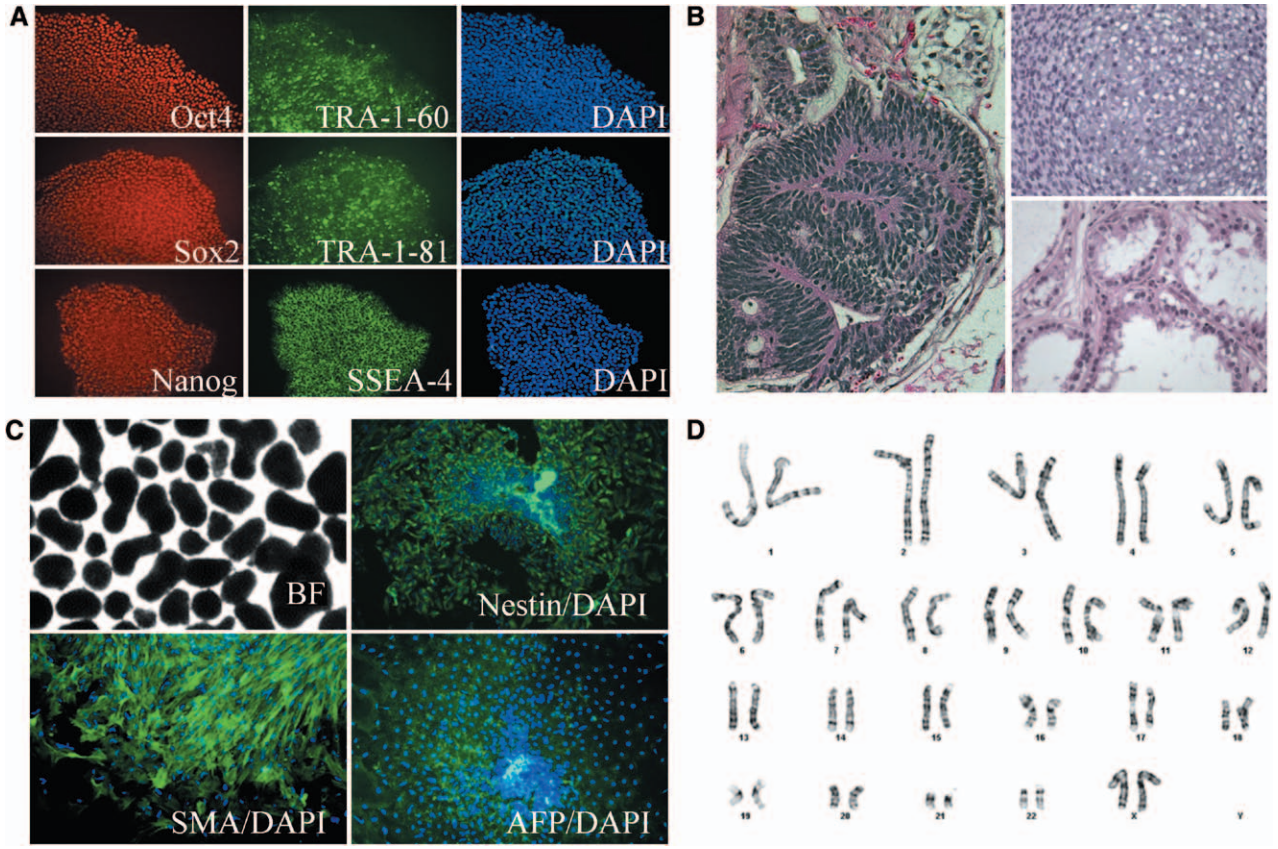

Figure 2. Pluripotency analysis of zinc finger nuclease (ZFN)–edited cells. A, ZFN-edited human embryonic stem cells (hESCs) expressed pluripotency markers that included Oct4, Tra-1–60, Sox2, Tra-1–81, Nanog, and SSEA4. Blue stainings (**right**) are 4'-6-diamidino-2-phenylindole (DAPI) staining of nuclei. **B**, ZFN-edited cells formed teratomas in vivo in immunodeficient mice. The teratomas contain all 3 germ layers, identified here as neural rosette ectoderm (**left**), cartilage mesoderm (**top right**), and gland endoderm (**bottom right**). **C**, ZFN-edited cells formed embryoid bodies (EBs) in vitro shown by brightfield (BF, **top left**) microscopic appearance and by expression of the neuroectoderm marker Nestin (**top right**), smooth muscle actin (SMA) mesoderm marker (**bottom left**), and α-fetoprotein (AFP) endoderm marker (**bottom right**). **D**, ZFN-edited hESC lines have a normal euploid karyotype.

differentiated into EBs, these EBs could still be imaged by BLI, demonstrating the retention of reporter gene expression after hESC differentiation (Figure 3C). As expected, ZFN-edited iPSCs also showed robust Fluc enzyme activity as gauged by BLI (Online Figure IVC and IVD). Finally, we demonstrated a strong correlation between the cell numbers and BLI signals (Figure 3D and 3E), validating the fact that Fluc signal intensity accurately represents the viable cell count. These results show that the quantity of ZFN-edited cells can be measured by BLI because the signal directly represents cell survival and proliferation. Similarly, we tested the activity of RFP for fluorescence imaging (Online Figure VA). In addition, we tested eGFP signal of the ZFN-edited a-myosin heavy chain (aMHC)-eGFP reporter cells. The edited iPSCs did not have eGFP signals at undifferentiated state (Online Figure VB). However, during CM differentiation, the eGFP signals can be detected on day 11 (Online Figure VC). The CMs start beating on day 12 (Online Video II). In summary, we have established that ZFN-driven targeted reporter addition into the AAVS1 locus in hESCs and iPSCs produces pluripotent cells and differentiated progenies that are robustly compatible with fluorescence, bioluminescence, and PET imaging.

ZFN-Edited Cells Maintain Long-Term Reporter Gene Expression

The key to being able to track cell fate is long-term transgene expression on addition to the AAVS1 locus. To determine whether the multifunctional reporter cassette maintains its transcriptional status in the AAVS1 locus over an extended period, we measured reporter gene activity every 7 days for up to 8 weeks after having obtained and validated the genome-edited single cell–derived clones. BLI analysis revealed that luciferase enzyme activity remained constant through the duration of the experiment, indicating the stability of our reporter gene expression in the ZFN-edited cells (Figure 3F and 3G).

In Vivo Imaging of ZFN-Edited Cells

Next, we examined the in vivo imaging potential of the ZFN-edited hESCs in mice. We injected 10^3, 10^4, 10^5, and 10^6 hESCs into a subcutaneous site of each mouse and performed BLI on day 2. The results revealed that as few as 10 000 cells could be efficiently detected in vivo (Figure 4A). The cell numbers and bioluminescence signals were correlated in vivo (Figure 4B), consistent with our in vitro results (Figure 3D and 3E). These results confirm that ZFN-edited cells are accurate in tracing cell behavior in vivo. To examine whether ZFN-edited hESCs can also be imaged in vivo long-term. we performed

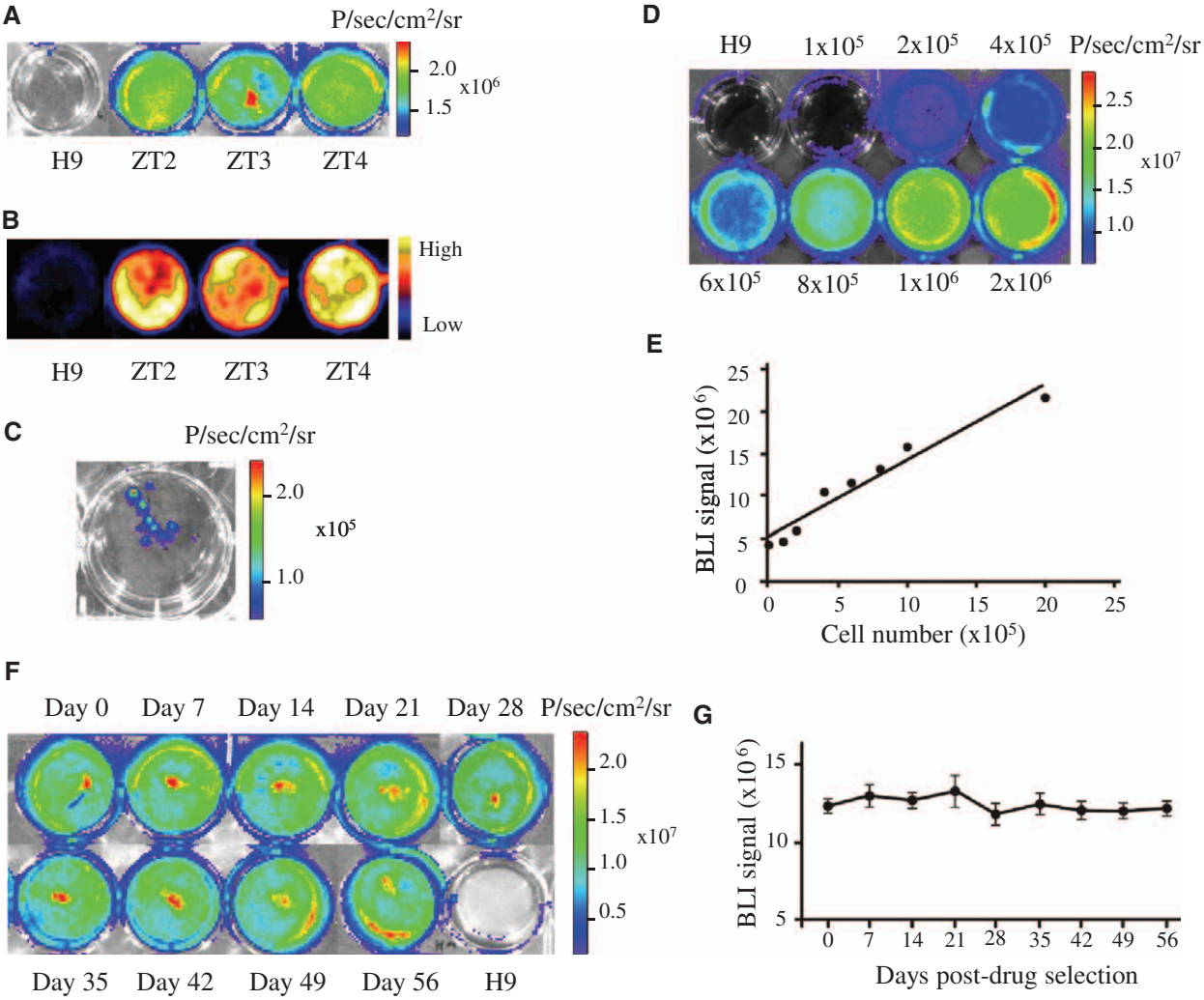

Figure 3. In vitro imaging of zinc finger nuclease (ZFN)–edited cells. Three ZFN-edited human embryonic stem cell (hESC) lines and a control unedited hESC line were monitored by (**A**) bioluminescence imaging (BLI) and (**B**) positron emission tomography imaging. **C**, ZFN-edited hESCs formed embryoid bodies and were then imaged by BLI. **D** and **E**, BLI analysis of ZFN-edited cells showed a linear correlation between cell number and BLI signals in vitro (R^2=0.95). **F** and **G**, To investigate the potential for epigenetic silencing of reporter gene expression, identical portions of ZFN-edited hESCs (after puromycin selection) were frozen from a continuously expanded batch every 7 days until day 56 when all portions were thawed in parallel and imaged by BLI puromycin (n=3). The BLI signals remained stable over time. Day 0 is the last day that cell culture was performed with drug selection.

a teratoma formation assay in immunodeficient mice. We successfully monitored the teratoma formation until sufficient palpability for explantation (until week 6) via BLI (Figure 4C and 4D). Therefore, the ZFN-edited cells and their derivatives are suitable for in vivo molecular imaging.

Molecular Imaging of Cardiomyocytes and Endothelial Cells Derived From ZFN-Edited ESCs

Myocardial infarction is the leading cause of death and morbidity in both industrialized and developing nations. Transplantation of cells, such as CMs and ECs, has shown promise as a strategy in the treatment of myocardial infarction.[36,38,39] However, the in vivo behavior of transplanted cells needs to be extensively investigated before clinical trials. To test the cardiovascular application potential of ZFN-edited cells, we first differentiated ZFN-edited hESCs into CMs (hESC-CMs) in vitro. We performed side-by-side comparisons of the ZFN-edited hESCs and unmodified hESCs for differentiation potential. After 12 days of differentiation, cell beating was observed for both ZFN-edited and unmodified hESC-CMs (Online Video III and IV). Both differentiation efficiency and cardiac marker expression (α-actinin, TNNT2, MLC-2a, and MLC-2v) in these ZFN-edited hESCs were similar to those seen in control unmodified hESCs (Online Figure VIA and VIB). Consistent with previous reports in hESCs and iPSCs,[40,41] 3 types of action potential morphologies (nodal-like, atrial-like, and ventricular-like) were recorded from unedited and edited hESC-CMs (Online Figure VIIA). The current-clamp mode recordings revealed no significant differences in action potential durations, action potential amplitudes, action potential durations at 90% repolarization, subpopulation ratio, or beating frequency between unedited and edited hESC-CMs (Online Figure VIIB–VIIF). Similarly, we differentiated ZFN-edited cells into ECs (hESC-ECs). Flow cytometry results showed ≈97% pure population ECs from ZFN-edited cells, and ≈96% pure population ECs

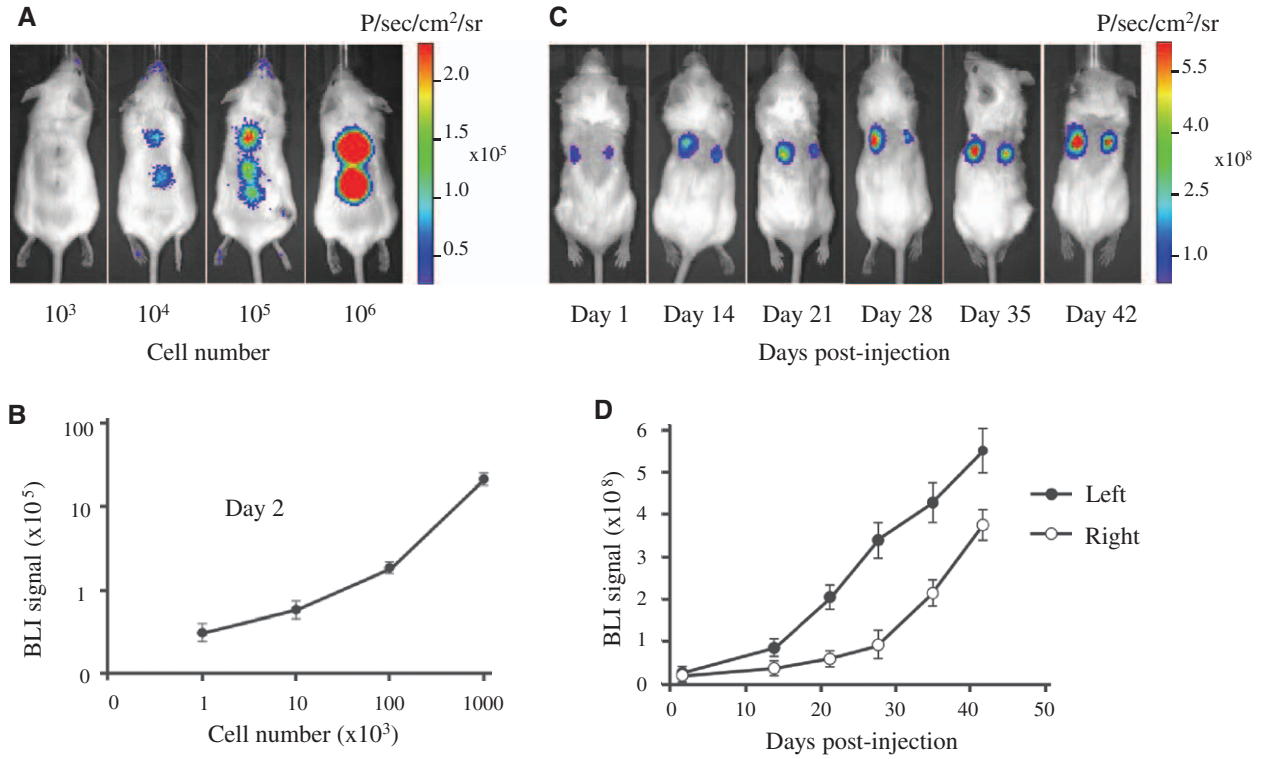

Figure 4. In vivo imaging of zinc finger nuclease (ZFN)–edited cells. A and **B**, Differing amounts of ZFN-edited human embryonic stem cells (hESCs) were injected into 2 distinct subcutaneous regions of mice and imaged by bioluminescence imaging (BLI) on day 2 (n=5). **C** and **D**, Teratomas formed by ZFN-edited cells were monitored by BLI up to 6 weeks. Left teratoma is indicated by filled circle; right teratoma is indicated by open circle.

from unmodified cells were obtained by assessment of endothelial marker CD31⁺ expression (Online Figure VIIIA). Morphogenesis, endothelial marker staining, angiogenesis potential, and DiI-ac-LDL uptake assays showed that ECs derived from ZFN-edited cells were also similar to those derived from control unmodified hESCs (Online Figure VIIIB–VIIID). These results demonstrate that the integration and expression of reporter genes from the AAVS1 locus do not influence the differentiation potential of hESCs.

Of further significant note, we show that 2 distinct differentiated cell types, CM and EC, generated from hESCs carrying a ZFN-directed transgenic cassette at AAVS1 are essentially indistinguishable from wild-type, unmodified, cells as gauged by a comprehensive panel of molecular and functional tests. We tested the imaging potential of these cells derived from ZFN-edited cells. As expected, both hESC-CMs and hESC-ECs showed robust luciferase signals by BLI in vitro (Figure 5A–5D). We then injected 1 million hESC-CMs or hESC-ECs into the mouse heart and imaged them in vivo. Robust luciferase signal was detected for both hESC-CMs and hESC-ECs in the heart up to 4 weeks after injection (Figure 5E–5H). The luciferase signal decreased over time as a result of donor cell death, consistent with results from our prior studies.[36,38,39] Overall, these results establish the applicability of ZFN-edited stem cells for preclinical in vitro and in vivo imaging studies.

Discussion

The present work aimed to use the latest genetic engineering techniques combined with in vitro and in vivo imaging applications to realize the full translational potential of hESCs and iPSCs. To our knowledge, this is the first application of ZFN genome editing technology for molecular imaging of hESCs and iPSCs. In this study, we successfully edited both hESCs and iPSCs using ZFNs and achieved a high efficiency of site-specific integration. We showed that both ZFN editing and reporter gene expression do not adversely affect cell pluripotency or differentiation potential for in vivo imaging applications. Furthermore, we demonstrated that over the extended period necessary for in vivo imaging, ZFN-edited cells robustly and stably expressed reporter genes without epigenetic silencing. Taken together, and in light of the recent advances in introducing stem cell progeny into the clinic, our data have important implications for the translational use of targeted genetic engineering.

First-generation transgenesis methods that rely on random integration are associated with substantial limitations. In this regard, we believe that ZFN-driven isogenic-targeted addition to a safe harbor is the preferred technology for basic science, preclinical, and in-the-clinic applications.[22,29] Our data agree with reports demonstrating that the AAVS1 locus is nonessential for hESC/iPSC pluripotency[29,31] and further establish that human stem cells carrying transgenes at this locus can be effectively imaged in vivo. We carefully compared, using a large panel of immunological, molecular, and cell physiological assays, the properties of unperturbed control cells and cells carrying a ZFN-directed transgene cassette at AAVS1. Both CMs and ECs transgenic at AAVS1 were indistinguishable from control nontransgenic cells in most aspects, other than being positive

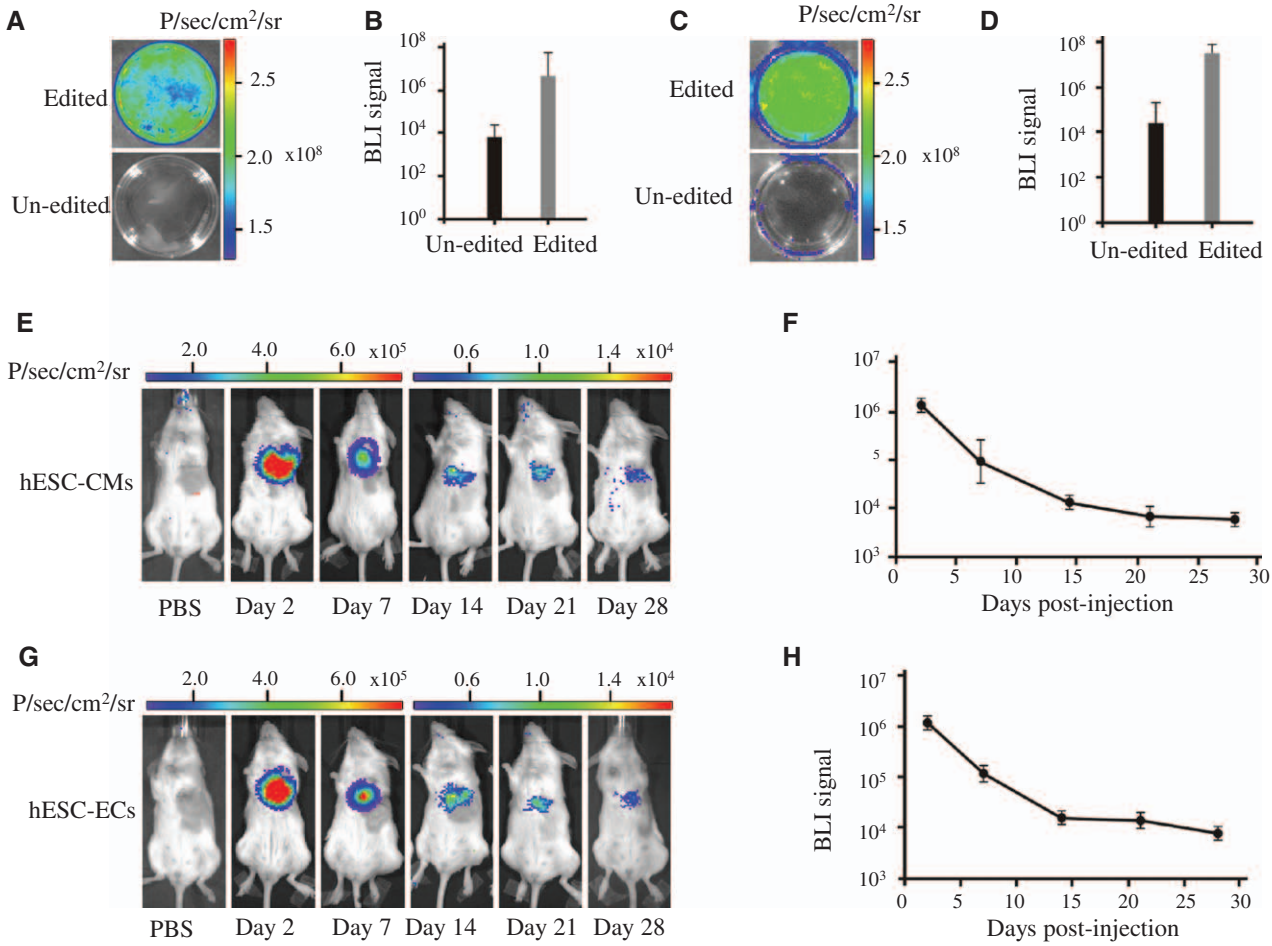

Figure 5. Molecular imaging of cardiomyocytes (CMs) and endothelial cells (ECs) derived from zinc finger nuclease (ZFN)–edited human embryonic stem cells (hESCs). A and **B**, CMs derived from ZFN-edited cells (**top**) showed robust bioluminescence imaging (BLI) signals, whereas CMs derived from unmodified H9 hESCs (**bottom**) showed no BLI signal (n=3). **C** and **D**, ECs derived from ZFN-edited H9 hESCs (**top**) showed robust BLI signals, whereas ECs derived from unmodified H9 hESCs (**bottom**) showed no signals (n=3). **E** and **F**, CMs derived from ZFN-edited cells were injected into the left ventricular myocardium of mice and imaged up to 4 weeks (n=5). **G** and **H**, ECs derived from ZFN-edited cells were injected into the left ventricular myocardium of mice and imaged up to 4 weeks (n=5).

for the transgene-encoding marker. Our data thus extend the existing data set on targeted gene addition to the AAVS1 locus[22,29,30,42] to demonstrate its suitability for in vivo imaging.

We built the reporter system not only to be multifunctional, but also to be compatible with a high-throughput process of engineering multiple distinct lines of hESCs and iPSCs. In our experiments, 100% of both hESC and iPSC single cell–derived marker-positive clones carried the reporter at the ZFN-specified location. Accuracy and efficiency of this sort reduce the workload-associated with isolating desired cells, obtaining 1 single cell–derived clone per reporter construct, and validating the clones before proceeding with downstream studies to the theoretically possible minimum. This means that the method we describe can be applied to large panels of hESCs and iPSCs without a measurable detriment to process flow. It is also important that the genetic approach is highly specific. The within-cell action profile of ZFNs we have engineered is a function of their DNA recognition specificity. We investigated a total of 27 maximal-likelihood off-target cleavage sites for the ZFNs we used[29] and found all to be wild type. Our data thus add to the existing body of evidence validating the in-cell specificity of these ZFNs.[29,43]

Molecular imaging plays an important role in the tracking of stem cell fate in vivo, but conventional vectors that randomly integrate reporter genes throughout the genome are problematic and have limited applicability. In fact, variable expression levels among transduced cells and genetic silencing within the cells may occur depending on the integration site of the reporter gene.[31,44,45] Thus, the conventional reporter gene–based imaging may not truly demonstrate the behavior of cells. In this study, we successfully achieved long-term stable gene expression for up to 2 months by integrating the reporter genes into the AAVS1 locus (ie, in isogenic settings). Our observations in this regard are consistent with results from previous studies in both transformed and stem cells.[22,29,42,45]

Pluripotent stem cells are capable of indefinite self-renewal and pluripotency and show promise for cell replacement therapy. However, to fully understand the beneficial effects of pluripotent stem cell therapy, investigators must be able to track the biology and physiology of transplanted cells in living subjects over time.[46] In previous studies, we transplanted hESC-ECs and hESC-CMs into murine myocardial infarction models and monitored cell fate using molecular imaging methods.[36,38,39] However, the expression of reporter genes in

these studies was achieved using a lentivirus system that could be silenced by epigenetic effects. To minimize the epigenetic influence, we made use of the ZFN-driven site-specific integration approach. CMs and ECs derived from ZFN-edited hESCs show no significant difference compared with those derived from unmodified ESCs, and the fate of these cells can be monitored in the heart over time. Application of this novel ZFN technology in the field of cardiovascular research can thus greatly accelerate the transition of findings from basic research toward clinical translation. In summary, our study has demonstrated that ZFN-driven addition of a reporter gene cassette is a powerful tool for modifying human pluripotent stem cells for molecular imaging.

Acknowledgments

We acknowledge Yongquan Gong for assistance with experimental protocols, Erica Moehle for drawing Figure 1A, and Philip Gregory for comments on the article. Requests for Zinc finger nucleases should be directed to F.D. Urnov (email: furnov@sangamo.com).

Sources of Funding

This work was supported, in part, by grants from Burroughs Wellcome Fund, Leducq Fondation, National Institutes of Health (NIH) DP2 OD004437, NIH EB009689, NIH HL113006, NIH HL093172, California Institute for Regenerative Medicine (CIRM) RB3-05129 (to J.C.W.), R01 HL095571 (to J.C.W.), U01 HL099776 (to R.C.R.), American Heart Association Beginning Grant-In-Aid 7660028 (to M.H.), and the International Society for Heart & Lung Transplantation (ISHLT) Research Fellowship Award (to P.E.A.).

Disclosures

F.D. Urnov is a full-time employee of Sangamo Biosciences, Inc. The other authors have no conflicts to report.

References

1. Thomson JA, Itskovitz-Eldor J, Shapiro SS, Waknitz MA, Swiergiel JJ, Marshall VS, Jones JM. Embryonic stem cell lines derived from human blastocysts. *Science*. 1998;282:1145–1147.
2. Takahashi K, Tanabe K, Ohnuki M, Narita M, Ichisaka T, Tomoda K, Yamanaka S. Induction of pluripotent stem cells from adult human fibroblasts by defined factors. *Cell*. 2007;131:861–872.
3. Yu J, Vodyanik MA, Smuga-Otto K, Antosiewicz-Bourget J, Frane JL, Tian S, Nie J, Jonsdottir GA, Ruotti V, Stewart R, Slukvin II, Thomson JA. Induced pluripotent stem cell lines derived from human somatic cells. *Science*. 2007;318:1917–1920.
4. Burridge PW, Keller G, Gold JD, Wu JC. Production of de novo cardiomyocytes: human pluripotent stem cell differentiation and direct reprogramming. *Cell Stem Cell*. 2012;10:16–28.
5. Narsinh K, Narsinh KH, Wu JC. Derivation of human induced pluripotent stem cells for cardiovascular disease modeling. *Circ Res*. 2011;108:1146–1156.
6. Dambrot C, Passier R, Atsma D, Mummery CL. Cardiomyocyte differentiation of pluripotent stem cells and their use as cardiac disease models. *Biochem J*. 2011;434:25–35.
7. Schwartz SD, Hubschman JP, Heilwell G, Franco-Cardenas V, Pan CK, Ostrick RM, Mickunas E, Gay R, Klimanskaya I, Lanza R. Embryonic stem cell trials for macular degeneration: a preliminary report. *Lancet*. 2012;379:713–720.
8. Ghosh Z, Huang M, Hu S, Wilson KD, Dey D, Wu JC. Dissecting the oncogenic and tumorigenic potential of differentiated human induced pluripotent stem cells and human embryonic stem cells. *Cancer Res*. 2011;71:5030–5039.
9. Cao F, Li Z, Lee A, Liu Z, Chen K, Wang H, Cai W, Chen X, Wu JC. Noninvasive de novo imaging of human embryonic stem cell-derived teratoma formation. *Cancer Res*. 2009;69:2709–2713.
10. Swijnenburg RJ, Schrepfer S, Cao F, Pearl JI, Xie X, Connolly AJ, Robbins RC, Wu JC. In vivo imaging of embryonic stem cells reveals patterns of survival and immune rejection following transplantation. *Stem Cells Dev*. 2008;17:1023–1029.
11. Barnett BP, Arepally A, Stuber M, Arifin DR, Kraitchman DL, Bulte JW. Synthesis of magnetic resonance-, X-ray- and ultrasound-visible alginate microcapsules for immunoisolation and noninvasive imaging of cellular therapeutics. *Nat Protoc*. 2011;6:1142–1151.
12. Ponomarev V. Nuclear imaging of cancer cell therapies. *J Nucl Med*. 2009;50:1013–1016.
13. Chen IY, Wu JC. Cardiovascular molecular imaging: focus on clinical translation. *Circulation*. 2011;123:425–443.
14. Nguyen PK, Lan F, Wang Y, Wu JC. Imaging: guiding the clinical translation of cardiac stem cell therapy. *Circ Res*. 2011;109:962–979.
15. Swijnenburg RJ, Schrepfer S, Govaert JA, Cao F, Ransohoff K, Sheikh AY, Haddad M, Connolly AJ, Davis MM, Robbins RC, Wu JC. Immunosuppressive therapy mitigates immunological rejection of human embryonic stem cell xenografts. *Proc Natl Acad Sci USA*. 2008;105:12991–12996.
16. Lee AS, Wu JC. Imaging of embryonic stem cell migration in vivo. *Methods Mol Biol*. 2011;750:101–114.
17. Sun N, Lee A, Wu JC. Long term non-invasive imaging of embryonic stem cells using reporter genes. *Nat Protoc*. 2009;4:1192–1201.
18. Krishnan M, Park JM, Cao F, Wang D, Paulmurugan R, Tseng JR, Gonzalgo ML, Gambhir SS, Wu JC. Effects of epigenetic modulation on reporter gene expression: implications for stem cell imaging. *FASEB J*. 2006;20:106–108.
19. Kita-Matsuo H, Barcova M, Prigozhina N, et al. Lentiviral vectors and protocols for creation of stable hESC lines for fluorescent tracking and drug resistance selection of cardiomyocytes. *PLoS ONE*. 2009;4:e5046.
20. Stein S, Ott MG, Schultze-Strasser S, et al. Genomic instability and myelodysplasia with monosomy 7 consequent to EVI1 activation after gene therapy for chronic granulomatous disease. *Nat Med*. 2010;16:198–204.
21. Ott MG, Schmidt M, Schwarzwaelder K, Stein S, Siler U, Koehl U, Glimm H, Kühlcke K, Schilz A, Kunkel H, et al. Correction of X-linked chronic granulomatous disease by gene therapy, augmented by insertional activation of MDS1-EVI1, PRDM16 or SETBP1. *Nat Med*. 2006;12:401–409.
22. DeKelver RC, Choi VM, Moehle EA, et al. Functional genomics, proteomics, and regulatory DNA analysis in isogenic settings using zinc finger nuclease-driven transgenesis into a safe harbor locus in the human genome. *Genome Res*. 2010;20:1133–1142.
23. de Souza N. Primer: genome editing with engineered nucleases. *Nat Methods*. 2012;9:27.
24. Urnov FD, Miller JC, Lee YL, Beausejour CM, Rock JM, Augustus S, Jamieson AC, Porteus MH, Gregory PD, Holmes MC. Highly efficient endogenous human gene correction using designed zinc-finger nucleases. *Nature*. 2005;435:646–651.
25. Santiago Y, Chan E, Liu PQ, Orlando S, Zhang L, Urnov FD, Holmes MC, Guschin D, Waite A, Miller JC, Rebar EJ, Gregory PD, Klug A, Collingwood TN. Targeted gene knockout in mammalian cells by using engineered zinc-finger nucleases. *Proc Natl Acad Sci USA*. 2008;105:5809–5814.
26. Moehle EA, Moehle EA, Rock JM, et al. Targeted gene addition into a specified location in the human genome using designed zinc finger nucleases. *Proc Natl Acad Sci USA*. 2007;104:3055–3060.
27. Carroll D. Genome engineering with zinc-finger nucleases. *Genetics*. 2011;188:773–782.
28. Zambrowicz BP, Imamoto A, Fiering S, Herzenberg LA, Kerr WG, Soriano P. Disruption of overlapping transcripts in the ROSA beta geo 26 gene trap strain leads to widespread expression of beta-galactosidase in mouse embryos and hematopoietic cells. *Proc Natl Acad Sci USA*. 1997;94:3789–3794.
29. Hockemeyer D, Soldner F, Beard C, et al. Efficient targeting of expressed and silent genes in human ESCs and iPSCs using zinc-finger nucleases. *Nat Biotechnol*. 2009;27:851–857.
30. Hockemeyer D, Wang H, Kiani S, et al. Genetic engineering of human pluripotent cells using TALE nucleases. *Nat Biotechnol*. 2011;29:731–734.
31. Smith JR, Maguire S, Davis LA, Alexander M, Yang F, Chandran S, ffrench-Constant C, Pedersen RA. Robust, persistent transgene expression in human embryonic stem cells is achieved with AAVS1-targeted integration. *Stem Cells*. 2008;26:496–504.
32. Lombardo A, Cesana D, Genovese P, et al. Site-specific integration and tailoring of cassette design for sustainable gene transfer. *Nat Methods*. 2011;8:861–869.

33. Wilson KD, Sun N, Huang M, Zhang WY, Lee AS, Li Z, Wang SX, Wu JC. Effects of ionizing radiation on self-renewal and pluripotency of human embryonic stem cells. *Cancer Res*. 2010;70:5539–5548.
34. Ray P, Tsien R, Gambhir SS. Construction and validation of improved triple fusion reporter gene vectors for molecular imaging of living subjects. *Cancer Res*. 2007;67:3085–3093.
35. Laflamme MA, Chen KY, Naumova AV, et al. Cardiomyocytes derived from human embryonic stem cells in pro-survival factors enhance function of infarcted rat hearts. *Nat Biotechnol*. 2007;25:1015–1024.
36. Li Z, Wilson KD, Smith B, Kraft DL, Jia F, Huang M, Xie X, Robbins RC, Gambhir SS, Weissman IL, Wu JC. Functional and transcriptional characterization of human embryonic stem cell-derived endothelial cells for treatment of myocardial infarction. *PLoS ONE*. 2009;4:e8443.
37. Jia F, Wilson KD, Sun N, Gupta DM, Huang M, Li Z, Panetta NJ, Chen ZY, Robbins RC, Kay MA, Longaker MT, Wu JC. A nonviral minicircle vector for deriving human iPS cells. *Nat Methods*. 2010;7:197–199.
38. Cao F, Wagner RA, Wilson KD, Xie X, Fu JD, Drukker M, Lee A, Li RA, Gambhir SS, Weissman IL, Robbins RC, Wu JC. Transcriptional and functional profiling of human embryonic stem cell-derived cardiomyocytes. *PLoS ONE*. 2008;3:e3474.
39. Li Z, Wu JC, Sheikh AY, Kraft D, Cao F, Xie X, Patel M, Gambhir SS, Robbins RC, Cooke JP, Wu JC. Differentiation, survival, and function of embryonic stem cell derived endothelial cells for ischemic heart disease. *Circulation*. 2007;116:I46–I54.
40. He JQ, Ma Y, Lee Y, Thomson JA, Kamp TJ. Human embryonic stem cells develop into multiple types of cardiac myocytes: action potential characterization. *Circ Res*. 2003;93:32–39.
41. Itzhaki I, Maizels L, Huber I, Zwi-Dantsis L, Caspi O, Winterstern A, Feldman O, Gepstein A, Arbel G, Hammerman H, Boulos M, Gepstein L. Modelling the long QT syndrome with induced pluripotent stem cells. *Nature*. 2011;471:225–229.
42. Lombardo A, Genovese P, Beausejour CM, Colleoni S, Lee YL, Kim KA, Ando D, Urnov FD, Galli C, Gregory PD, Holmes MC, Naldini L. Gene editing in human stem cells using zinc finger nucleases and integrase-defective lentiviral vector delivery. *Nat Biotechnol*. 2007;25:1298–1306.
43. Zou J, Sweeney CL, Chou BK, Choi U, Pan J, Wang H, Dowey SN, Cheng L, Malech HL. Oxidase-deficient neutrophils from X-linked chronic granulomatous disease iPS cells: functional correction by zinc finger nuclease-mediated safe harbor targeting. *Blood*. 2011;117:5561–5572.
44. Ellis J. Silencing and variegation of gammaretrovirus and lentivirus vectors. *Hum Gene Ther*. 2005;16:1241–1246.
45. Ramachandra CJ, Shahbazi M, Kwang TW, Choudhury Y, Bak XY, Yang J, Wang S. Efficient recombinase-mediated cassette exchange at the AAVS1 locus in human embryonic stem cells using baculoviral vectors. *Nucleic Acids Res*. 2011;39:e107.
46. Cao F, Lin S, Xie X, Ray P, Patel M, Zhang X, Drukker M, Dylla SJ, Connolly AJ, Chen X, Weissman IL, Gambhir SS, Wu JC. In vivo visualization of embryonic stem cell survival, proliferation, and migration after cardiac delivery. *Circulation*. 2006;113:1005–1014.

Novelty and Significance

What Is Known?

- Molecular imaging plays an important role in the characterization of stem cell behavior inside living organisms.
- Zinc finger nuclease (ZFN) technology bypasses the negative effects of current random genetic integration techniques.
- The AAVS1 locus is a safe harbor site in human genome and supports long-term transgene expression.

What New Information Does This Article Contribute?

- Use of ZFN to introduce the triple fusion reporter gene into the safe harbor AAVS1 locus for effective molecular imaging.
- Combines the latest genetic engineering techniques with state-of-the-art in vitro and in vivo imaging applications to create a platform for investigating the translational potential of human embryonic stem cells and induced pluripotent stem cells.

Currently, most stable reporter gene expression is based on random integration, which is associated with unwanted insertional mutations and harmful effects on genetic expression, rendering this method problematic for clinical translation. The present work aimed to use the latest genome editing technique with molecular imaging applications to bypass these negative consequences and facilitate future translational potential of human embryonic stem cells and induced pluripotent stem cells. Using ZFN technology, we integrated a reporter gene complex into the AAVS1 locus of multiple pluripotent cell lines, injected these pluripotent cell progeny in mouse models, and tracked cell fate in vivo using bioluminescence imaging. We carefully compared these edited pluripotent cell lines and their derivatives, using a large panel of immunological, molecular, cellular, and physiological assays, with unmodified control cells to verify that our ZFN-modified cells are indistinguishable from control cells. Our data extend the existing data set on novel application of ZFN technology to targeted genetic engineering for molecular imaging of human pluripotent stem cells and their progeny. Genome editing on safe harbor sites may be a powerful technology for basic and translational research in cardiovascular sciences.

SUPPLEMENTAL METHODS

Derivation of human iPSC lines. For human iPSC generation, we followed the protocol developed by Jia et al.[1] Briefly, human adipose stem cells (ASCs) were collected from the adipose tissue of a consenting 50-year old female undergoing elective lipo-aspiration via VASER Lipo System (Sound Surgical Technologies), in accordance with Stanford University human IRB guidelines. At the time of the operation, the patient had neither prior evidence nor knowledge of continuing systemic diseases. During the operation, the excised tissues specimen was immediately placed on ice and consecutively washed in serial dilutions of dilute Betadine, and then by two PBS (pH 7.2) washes of equal volume. Digestion of the adipose tissues was performed using equal volume of 0.075% (wt/vol) type II collagenase in Hank's balanced salt solution (Sigma-Aldrich) and agitated in a 37°C water bath at 125 rpm for 30 min, after which the stromal vascular fraction was pelleted by centrifugation (1,200*g* for 5 min) post collagenase inactivation. The pellet was resuspended, filtered through a 100 μm cell strainer, and plated onto gelatin-coated 15 cm dishes for proliferation. For reprogramming the ASCs, program "U-023" of the Nucleofector Kit R (Amaxa) was used for nucleofection of the reprogramming plasmid *P2PhiC31-LGNSO* (following the manufacturer's protocol), and the transfected cells were plated onto 10 cm dishes. Cells were cultured in DMEM/F12 medium (Invitrogen) supplemented with 10% FBS, 110 mg/L sodium pyruvate, Glutamax-I, 4.5g/L glucose, 50 μg/ml streptomycin, and 50 units/ml penicillin at 37^{o}C, 95% air, and 5% CO2 in a humidified incubator. Successfully transfected cells (GFP-positive) were sorted out by flow cytometry 3 days post-transfection, seeded onto gelatin-coated 6-well plates, and switched to hESC culture medium one day after seeding; medium changes were performed every 2 days. Using Lipofectamine 2000 (Invitrogen),

we then transfected the cells again with minicircles on days 4 and 6. After 18 days, we observed colonies that clearly displayed morphologies similar to those of hESC colonies.

Genomic polymerase chain reaction (PCR) to detect reporter gene addition. Single colonies were picked and genomic DNA was extracted using QuickExtract (Epicentre) following the online protocol. To detect the reporter gene addition, nested PCR was performed; 2 μl of genomic DNA was used for the PCR. The primers used in the first round of PCR were AAVScaggs-1F/AAVS-1R; primers in the second round of PCR were AAVScaggs-2F/AAVS-2R (see Online Table I). The PCR program was 94°C for 30 s and 35 cycles of 94°C for 30 s, 58°C for 30 s, and 72°C for 30 s. The PCR program for the nested PCR was 94°C for 30 s and 30 cycles of 94°C for 30 s, 62°C for 30 s, and 72°C for 15 s.

Teratoma formation assay. For tracking *in vivo* teratoma formation, one million ZFN-edited hESCs were suspended in 25 μL PBS, mixed with equal volumes of Matrigel, and injected into the subcutaneous regions of the backs of immunodeficient, female SCID mice (n=2 spots per group of mice) (Charles River Laboratories, Wilmington, MA). Fifty days after transplantation, teratomas were explanted, and histological staining was performed to assay cell differentiation. Teratomas were fixed with 4% paraformaldehyde, set in paraffin, sectioned, and stained with hematoxylin & eosin (H&E). Light microscopy was then used to visualize the sections.

PCR to detect non-homologous end joining (NHEJ) modification of AAVS1 locus. Genomic DNA from each cell line was extracted using QuickExtract (Epicentre) following their online protocol. 2 μl of genomic DNA was used for the PCR. The primers used in the first round of

PCR were AAVS1cut-F / AAVS1_rev_Cel1; primers in the second round of PCR were AAVS1_fwd_Cel1/ AAVS1cut-R (see Online Table I). The PCR program was 94°C for 30 s and 35 cycles of 94°C for 30 s, 58°C for 30 s, and 72°C for 30 s. The PCR program for the nested PCR was 94°C for 30 s and 30 cycles of 94°C for 30 s, 62°C for 30 s, and 72°C for 15 s.

Embryoid body (EB) formation. hESCs and iPSCs were collected by collagenase IV treatment (1 µg/ul), resuspended in 20%FBS/DMEM media and allowed to form EBs in a six-well plate (Costar 3471) for up to 2 weeks. The EBs were then broken down into smaller clumps using a 200 µl pipet tip and allowed to attach onto gelatin-coated plates for an additional 2 days, followed by fixing and staining for the three embryonic germ layers and trophectoderm.

Pluripotency markers and EB analysis. hESC and iPSC colonies plated on 6-well tissue culture plates (Sigma Aldrich, St. Louis, MO) were fixed in 4% paraformaldehyde at room temperature for 5 minutes and then permeabilized with 1 mL of 0.5% triton for 10 min. After washing with PBS, cells were incubated with primary antibody (1:100 in PBS) at room temperature for 1 h. The primary antibodies used for staining were Oct3/4 (Santa Cruz Biotechnology), Sox2 (Biolegend), SSEA-4 (Chemicon), Tra-1–60 (Chemicon), Tra-1–81 (Chemicon), and Nanog (Santa Cruz Biotechnology). After thorough washing with PBS (3 x 5min), AlexaFluor-conjugated secondary antibodies at a dilution of 1:250 (Santa Cruz Biotechnology) were added for 20 min. To highlight the nuclei, DAPI (1:200) was added together with secondary antibody. After 3 washes with PBS, immunofluorescent images were taken by fluorescent microscopy.

Fluorescence activated cell sorting (FACS) of ZFN-modified hESC-ECs. The resulting human EBs were then dissociated into single cells by treatment with 0.25% collagenase I (Invitrogen, Carlsbad, CA) for 30 min at 37^{o}C, then with 0.56 units/ml Liberase Blendzyme IV (Roche Diagnostics, Indianapolis) for 10–20 minutes at 37^{o}C. Cells were subsequently strained through a 40-mm cell strainer (BD Falcon, San Diego) and incubated with rabbit anti-human CD144 (Abcam, Cambridge, MA) and mouse anti-human CD31 (BD). Using FACScan (Becton Dickinson), $CD144^{+}/CD31^{+}$ cells were sorted out and grown on 4 g/cm2 human fibronectin coated plates (Calbiochem, San Diego, CA) with EGM- 2 (Lonza), 5% Knockout SRTM, and 5 ng/ml VEGF. Medium was replenished every 2–3 days.

Animal surgery for delivery of hESCs, CMs, or ECs into the heart. To validate imaging of the derived cells, we transplanted the hESCs, hESC-CMs and hESC-ECs into murine hearts. All animal protocols received prior approval from the Stanford Animal Research Committee. An experienced microsurgeon delivered $1x10^{6}$ of ZFN-edited hESCs, or ZFN-edited hESC-CMs as well as hESC-ECs (separately) in 30 μl of PBS into the left ventricular myocardium (n=3 for each cell type). The procedures were performed on young (7-9 weeks old) female immunodeficient SCID mice (Charles River Laboratories). Animals were anesthetized using 2% isoflurane and constantly monitored. Intubation, ventilation, and anesthetization were done with isoflurane (1% to 2%). A 24-hour recovery period on 37^{o}C heat pads was given post-surgery, after which the mice appeared to be fully active. The mortality rate was 0%.

Bioluminescence imaging (BLI) for longitudinal tracking of cell fate. To visualize survival and proliferation *in vivo*, mice underwent BLI using the Xenogen In Vivo Imaging System

(Caliper, Alameda, CA). Reporter probe D-Luciferin (375 mg/kg) was injected intraperitoneally 15 minutes ahead of image acquisition, and animals were imaged for 35 minutes using 1-second intervals of acquisition. Using Igor image analysis software (Wavemetrics, Lake Oswego, OR), regions of interest (ROIs) were drawn over the areas of localized signals and were standardized for both acquisition time and quantified in units of maximum photons per second per square centimeter per steradian (photons/sec/cm^2/sr) as previously described[2]. Imaging time points were conducted on days 1, 4, 7, 14, 21, 28, 35, 42, 49, and 56 post-injection.

Positron emission tomography (PET) imaging for longitudinal tracking of small fate. A microPET R4 rodent model scanner (Siemens Medical Solutions) was used to perform PET imaging on animals injected with AAVSI-TF H9 lines. Animals were anesthetized with 1-2% isoflurane, injected intravenously with 98±13 μCi of reporter probe 9-4-[^{18}F]fluoro-3-(hydroxymethyl) butyl]guanine ([^{18}F]FHBG), and scanned for 5 minutes after waiting 1 hour post injection. A two-dimensional ordered subsets expectation maximum (2D-OSEM) algorithm was used to reconstruct the images as previously described[2].

SUPPLEMENTAL VIDEOS

Online Video I. EBs formed from ZFN-edited hESCs attached onto tissue plates and showed spontaneous beating.

Online Video II. Cardiomyocytes derived from MHC-eGFP-edited iPSCs started beating after 11 days differentiation.

Online Video III. Cardiomyocytes derived from ZFN-edited hESCs started beating after 12 days differentiation.

Online Video IV. Cardiomyocytes derived from un-edited hESCs started beating after 12 days differentiation.

SUPPLEMENTAL FIGURE LEGEND

Online Figure I. Analysis of the putative off-target cleavage induced by AAVS1 ZFNs. (A) Southern blot analysis of random ZFN expression vector integration. For standard controls, digested human genomic DNA was spiked with 600bp DNA fragment from ZFN expression vector to correspond to 100, 20, 5, and 1 copies per diploid genome. The same DNA fragment was used as a probe to detect the potential random expression vector in ZFN-edited cell lines. Un-edited H9 cells were used as negative controls. The 28S rDNA was probed as a loading control. **(B-C)** Nine SELEX-predicted genomic off-targets were PCR-amplified and sequenced for three ZFN-edited cell lines and a control H9 cell line as indicated. None of these three clones showed any mutations in the potential off-target sequences. Numbers 2, 3, and 4 at the bottom of the figure indicate clones ZT2, ZT3, and ZT4, respectively. The size of PCR bands was shown on the left. OT: off-target. (**D-E)** The empty AAVS1 allele in clone ZT4 was wild-type, analyzed by PCR and subsequent DNA sequencing. **(F)** The reporter gene addition of the ZFN-edited H7 cell pool was confirmed by PCR.

Online Figure II. iPSC characterization and ZFN-driven reporter gene addition. (A) Human iPSCs generated from hASCs expressed pluripotency markers that included OCT4, Tra-1-60, SOX2, Tra-1-81, NANOG, and SSEA4. Blue staining (right panels) are DAPI staining of nuclei. **(B)** iPSCs formed teratomas *in vivo* in immunodeficient mice that include all 3 germ layers, identified here as cartilage mesoderm (left), neural rosette ectoderm (middle), and gland endoderm (right). **(C)** iPSCs formed embryoid bodies (EBs) *in vitro* shown by bright field (BF, top left) microscopic appearance, and by expression of Nestin neuroectoderm marker (top right), smooth muscle actin (SMA) mesoderm marker (bottom left), and α-fetoprotein (AFP) endoderm

marker (bottom right). **(D)** Six iPSC clones were screened by genomic PCR and all of them contained site-specific integration. The control cells were transfected with donor DNA without ZFNs, and thus did not produce any amplified bands. **(E)** Schematic diagram of MHC-eGFP plasmid. This reporter gene was used to report the cardiomyocyte differentiation. **(F)** The reporter gene addition to the four ZFN-edited iPSC lines was confirmed by PCR.

Online Figure III. Morphology of ZFN-edited hESCs. ZFN-edited hESCs formed tightly packed colonies with morphologies similar to un-edited H9 cells**.** Three typical colonies for each cell line are shown here.

Online Figure IV. Characterization of ZFN-edited human iPSCs. (A) ZFN-edited iPSCs expressed pluripotency markers OCT4, Tra-1-60, SOX2, Tra-1-81, NANOG, and SSEA4. Right panels are DAPI staining of nuclei; **(B)** ZFN-edited iPSCs form EBs *in vitro* shown by brightfield microscopic appearance (top left), and by expression of Nestin neuroectoderm marker (top right), smooth muscle actin (SMA) mesoderm marker (bottom left), and α-fetoprotein (AFP) endoderm marker (bottom right). **(C)** BLI was performed to test the enzyme activities of luciferase enzyme in four selected single cell-derived ZFN-modified iPSC lines with relatively more embryonic stem cell-like morphology. **(D)** BLI was performed to test the enzyme activities of luciferase enzyme in three ZFN-edited iPSC pools. The un-edited JL cell line was used as a negative control.

Online Figure V. Analysis of RFP gene in HEK 293 cells and eGFP gene in the MHC-eGFP modified iPSC line. (A) After transient expression of triple fusion reporter genes in HEK

293 cells, the RFP signals could be detected by microscope. Left panel: bright field; right panel: fluorescence. **(B)** MHC-eGFP modified iPSC line does not show eGFP signal, indicating cardiomyocyte specific promoter MHC does not leak. **(C)** eGFP signal can be detected in the MHC-eGFP modified iPSC-derived cardiomyocytes,

Online Figure VI. Comparison of CMs derived from human ZFN-edited and un-edited ESCs. (A) ZFN-edited (left) and un-edited (right) hESCs showed similar cardiomyocyte differentiation ability, as measured by immunostaining of TNNT2. **(B)** ZFN-edited (top) and un-edited (bottom) hESCs showed similar morphogenesis and cardiomyocyte marker expression. The bright field (BF) image is a beating cardiomyocyte clump. CMs express cardiac specific markers such as α-actinin (green), TNNT2 (red), MLC2a (red), and MLC2v (red). The enlarged field shows the striation of the CM. Cell nuclei were stained with DAPI (blue). Scale bar=50 μM.

Online Figure VII. Electrophysiological characterization of un-edited hESC-CMs and edited hESC-CMs. (A) Single spontaneous action potentials from representative un-edited hESC-CMs (upper panel) and edited hESC-CMs (lower panel) indicating presence of myocytes exhibiting nodal, atrial, and ventricular waveforms in current clamp mode. Dashed lines show 0 mV. **(B)** Quantification of nodal, atrial, and ventricular resting membrane potentials in un-edited hESC-CMs and edited hESC-CMs. **(C)** Quantification of nodal, atrial, and ventricular action potential amplitudes (APA) in un-edited hESC-CMs and edited hESC-CMs. **(D)** Quantification of nodal, atrial, and ventricular action potential durations at 90% repolarization (APD_{90}) in un-edited hESC-CMs and edited hESC-CMs. **(E)** Quantification of nodal, atrial, and ventricular

sub-populations in un-edited hESC-CMs and edited hESC-CMs. Note the lack of significant differences in resting potential (panel B), APA (panel C), APD_{90} (panel D) or sub-population ratios (panel E) between un-edited hESC-CMs and edited hESC-CMs. **(F)** Quantification of nodal, atrial, and ventricular beating frequency. There are no differences in beating frequencies between un-edited hESC-CMs and edited hESC-CMs.

Online Figure VIII. Comparison of ECs derived from ZFN-edited and un-edited hESCs. **(A)** Immunostaining of CD31 revealed that 97% EC purity from ZFN-edited hESCs and 96% EC purity from un-edited hESCs were achieved after sorting. **(B)** ECs derived from ZFN-edited (top) and un-edited (bottom) cells express endothelial specific markers CD31 (green) and CD144 (red). Cell nuclei were stained with DAPI (blue). **(C)** Endothelial tube formation by ZFN-edited (top) and un-edited (bottom) ECs after 48 hours of plating. **(D)** The ZFN-edited (top) and un-edited (bottom) ECs showed similar DiI-ac-LDL (DiI-acetylated low-density lipoprotein) uptake (red).

SUPPLEMENTAL REFERENCES

1. Jia F, Wilson KD, Sun N, Gupta DM, Huang M, Li Z, Panetta NJ, Chen ZY, Robbins RC, Kay MA, Longaker MT, Wu JC. A nonviral minicircle vector for deriving human ips cells. *Nat Methods*. 2010;7:197-199
2. Cao F, Lin S, Xie X, Ray P, Patel M, Zhang X, Drukker M, Dylla SJ, Connolly AJ, Chen X, Weissman IL, Gambhir SS, Wu JC. In vivo visualization of embryonic stem cell survival, proliferation, and migration after cardiac delivery. *Circulation*. 2006;113:1005-1014
3. Hockemeyer D, Soldner F, Beard C, Gao Q, Mitalipova M, DeKelver RC, Katibah GE, Amora R, Boydston EA, Zeitler B, Meng X, Miller JC, Zhang L, Rebar EJ, Gregory PD, Urnov FD, Jaenisch R. Efficient targeting of expressed and silent genes in human escs and ipscs using zinc-finger nucleases. *Nat Biotechnol*. 2009;27:851-857

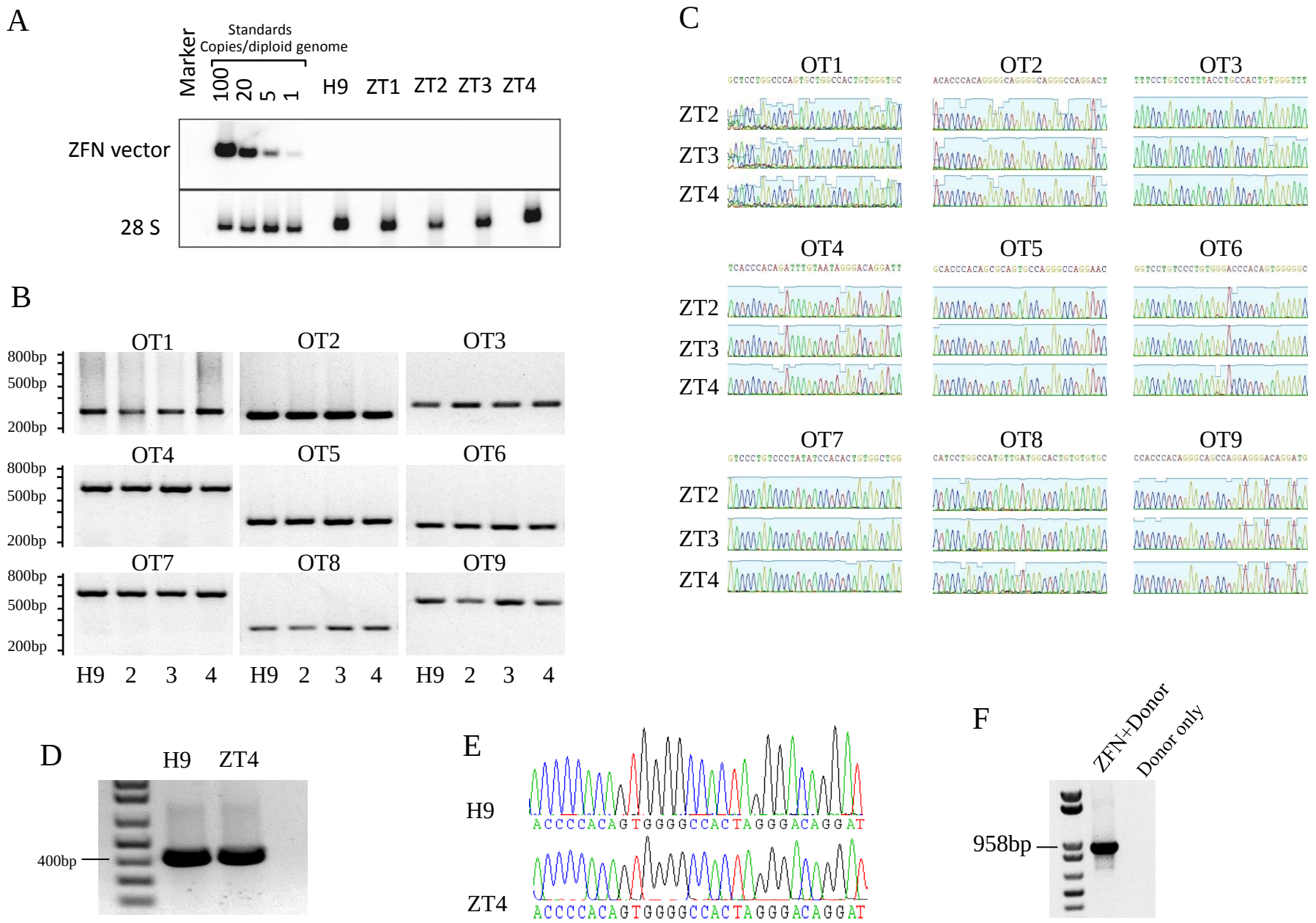

Online Figure I

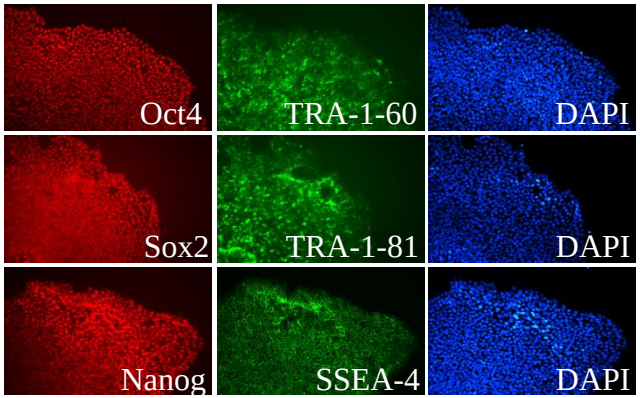

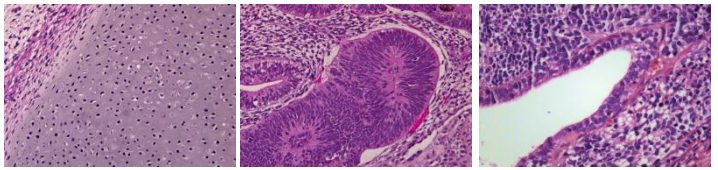

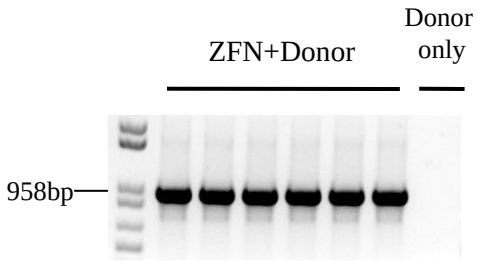

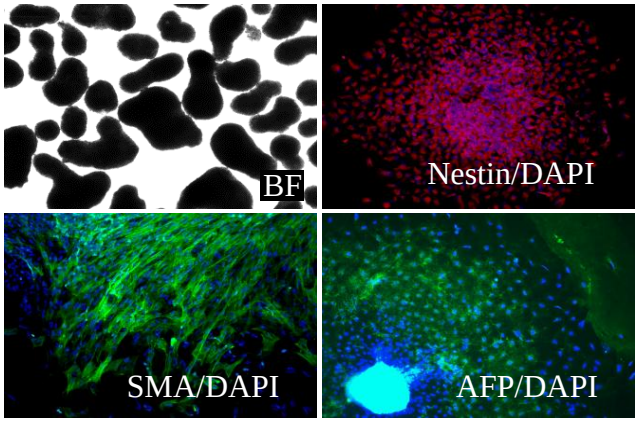

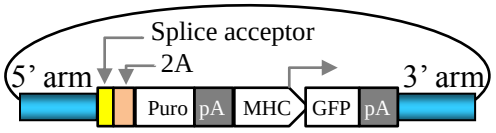

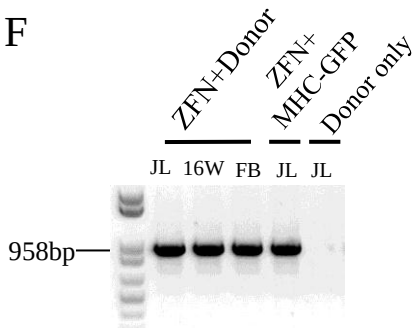

Online Figure II

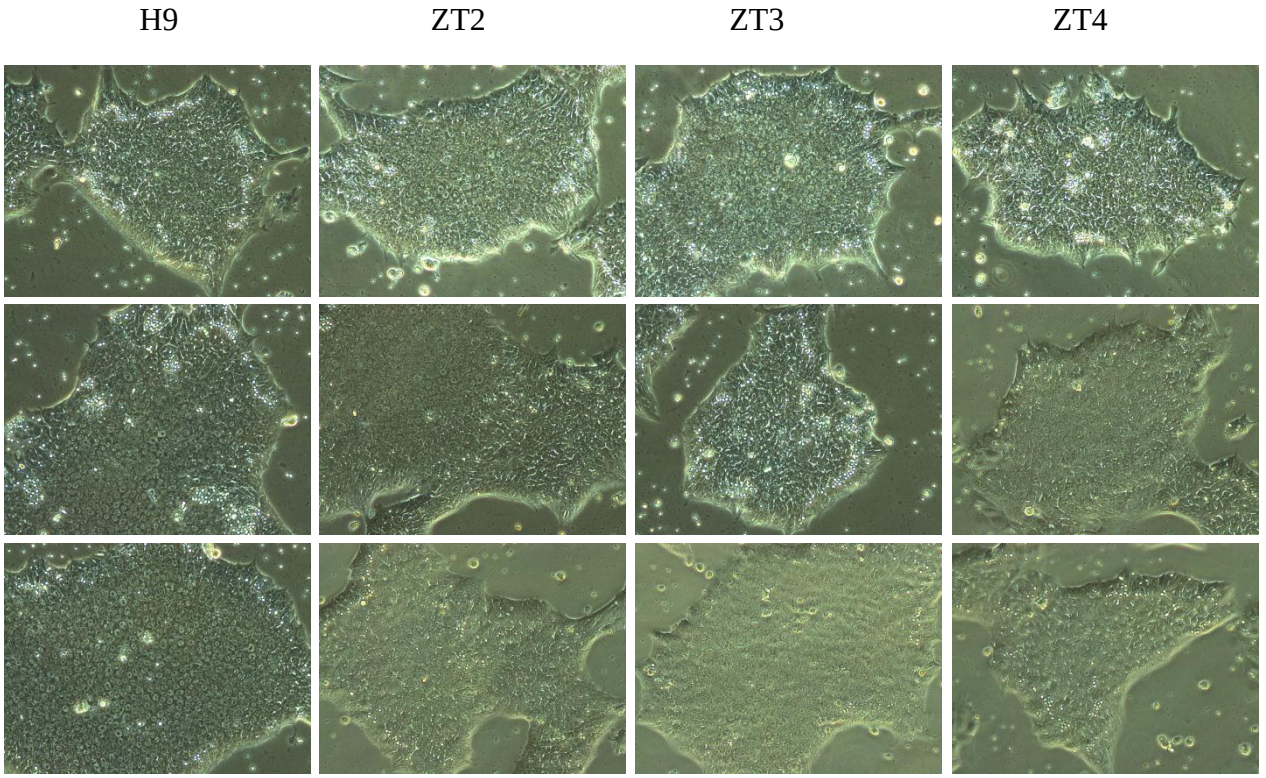

Online Figure IH

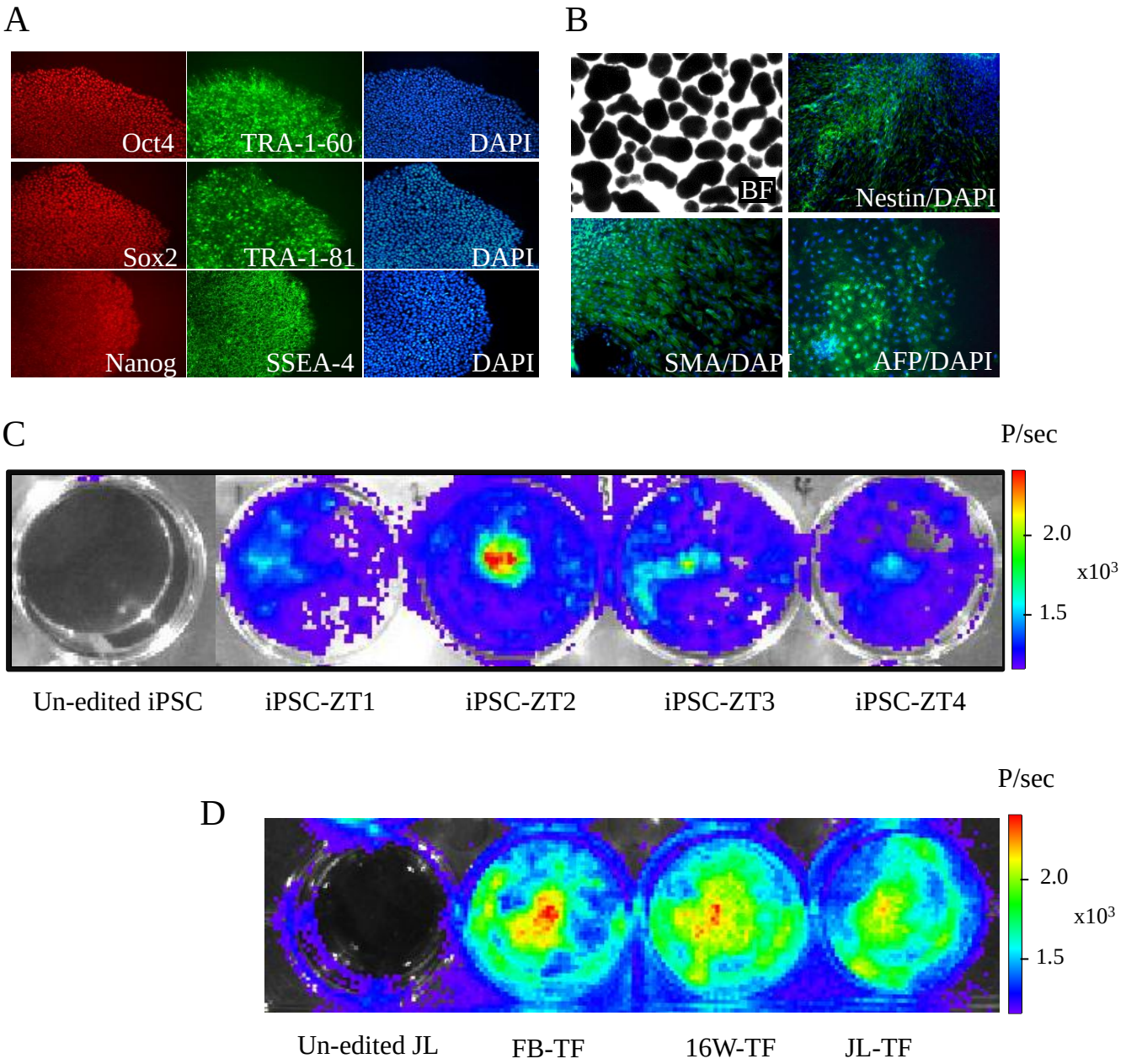

Online Figure IV

A

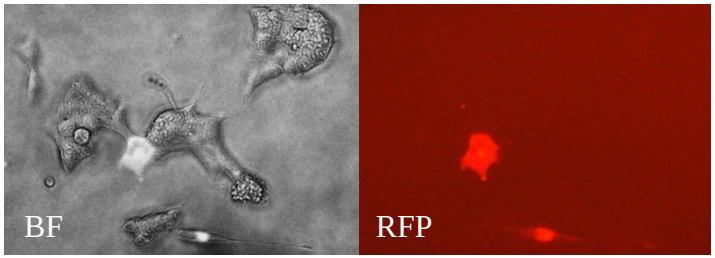

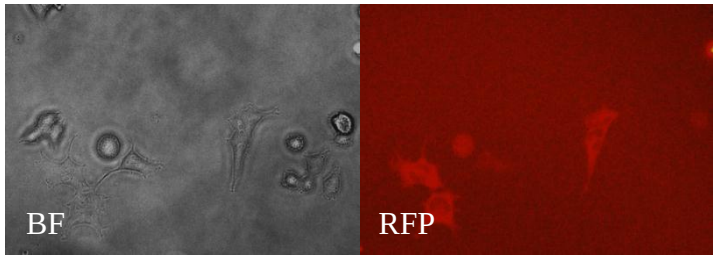

B

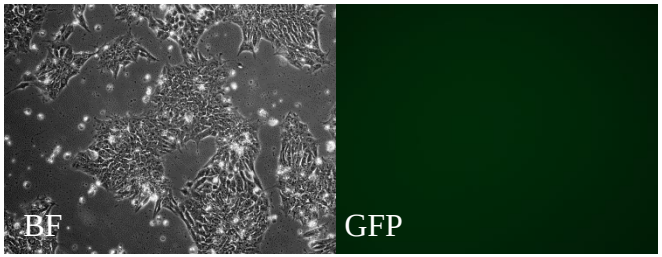

C

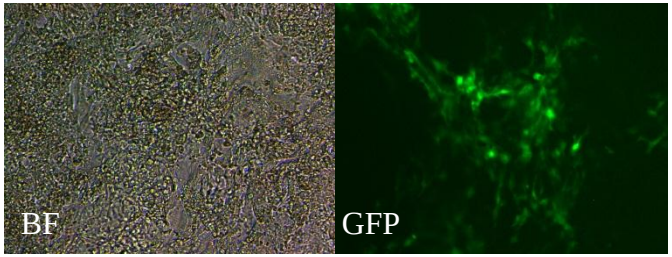

Online Figure V

A

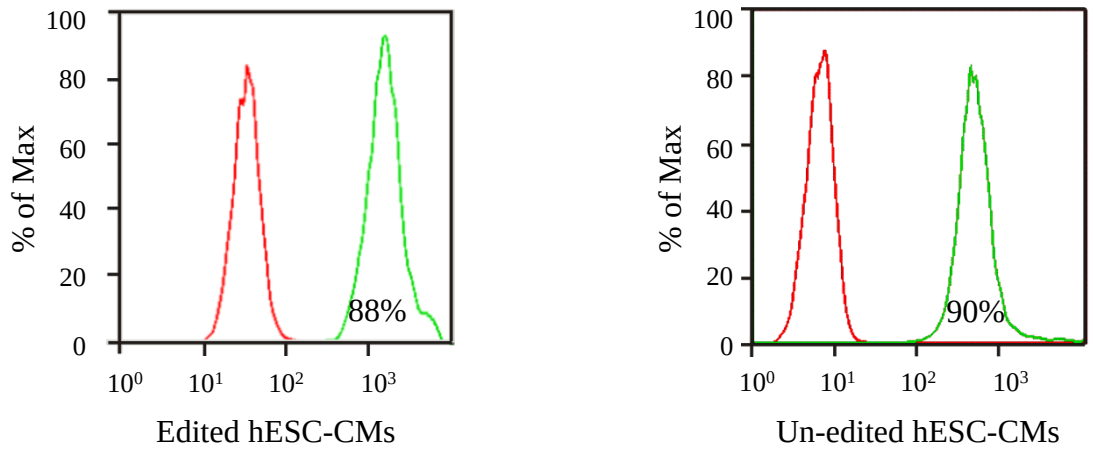

B

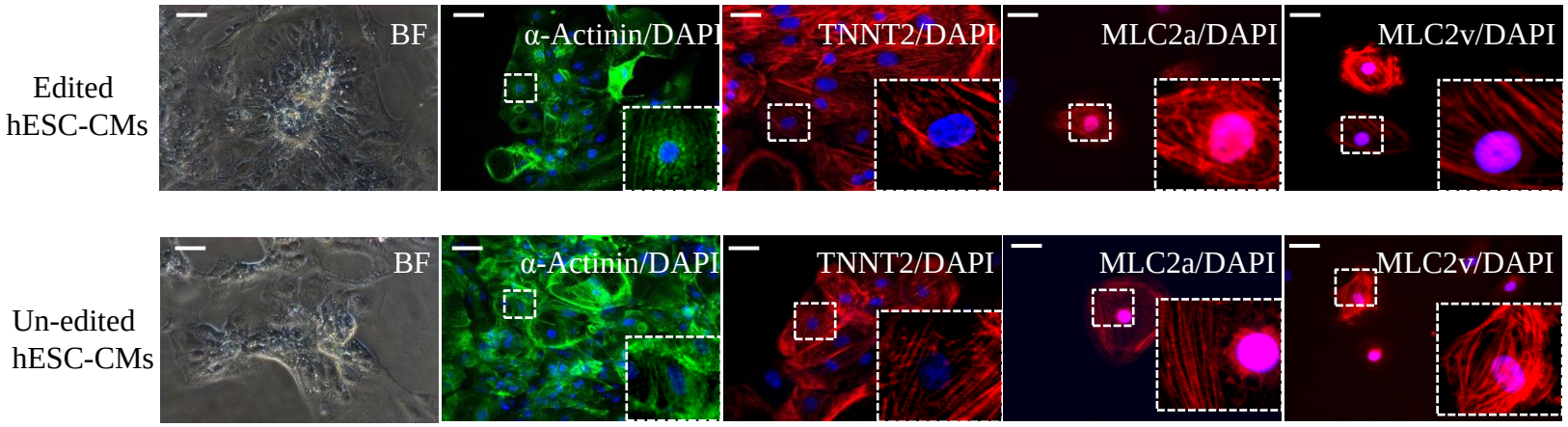

Online Figure VI

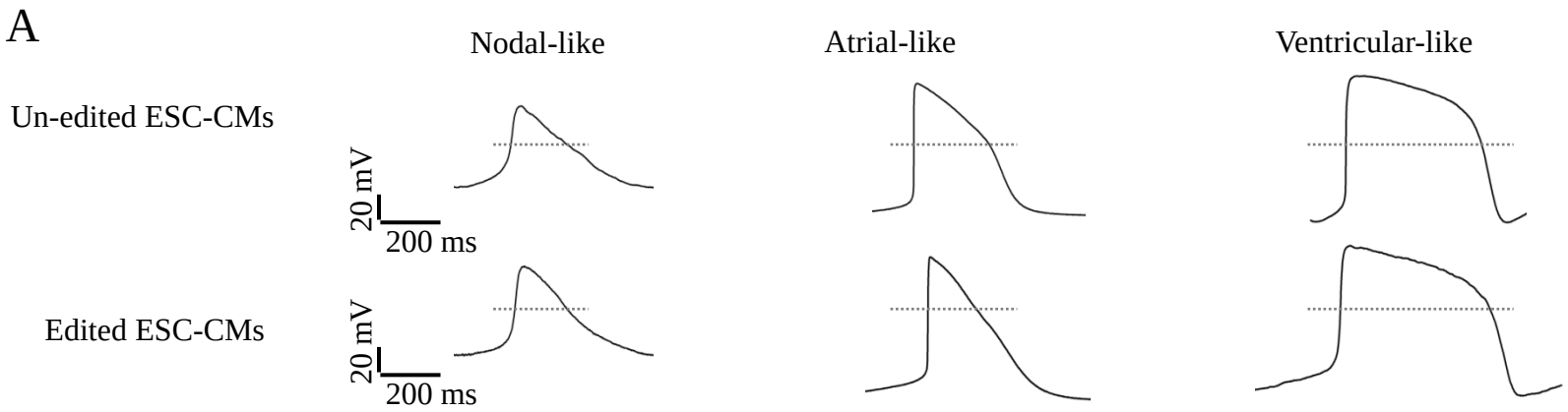

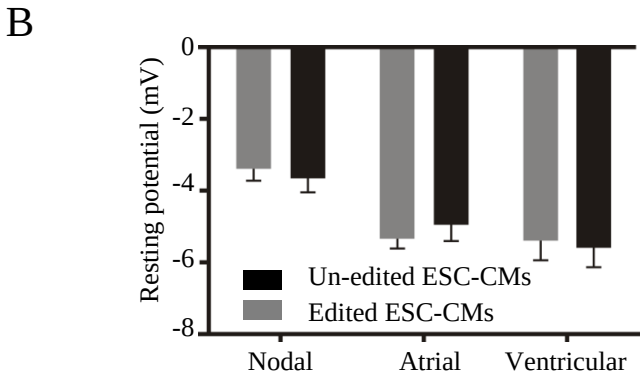

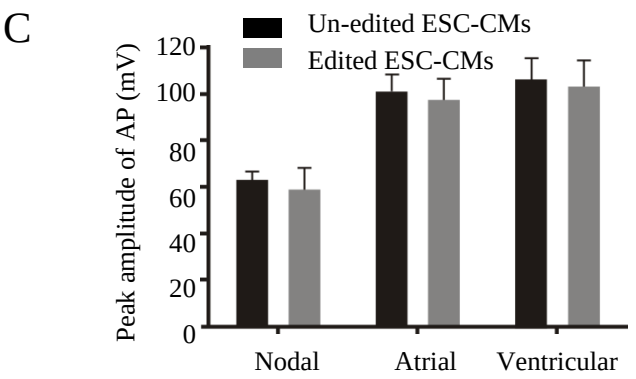

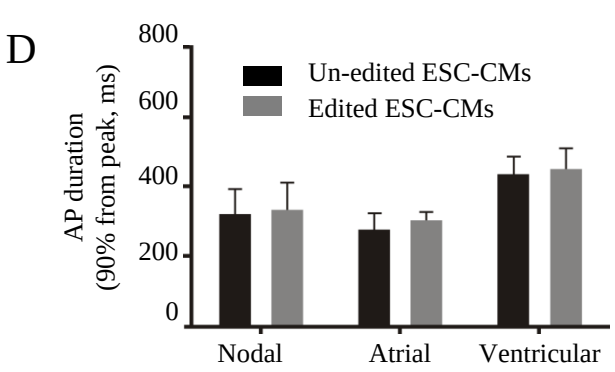

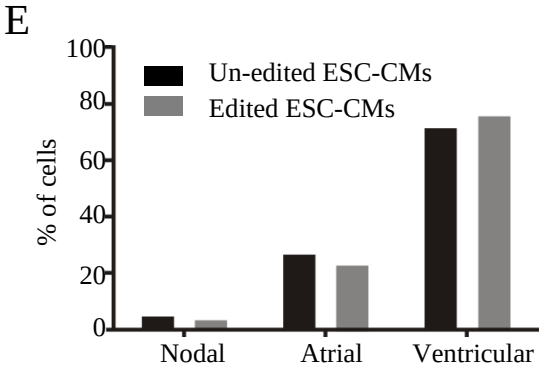

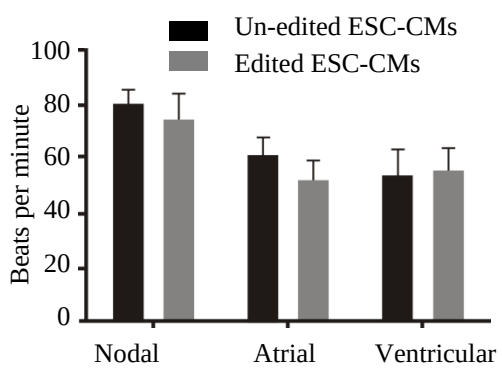

Online Figure VII

A

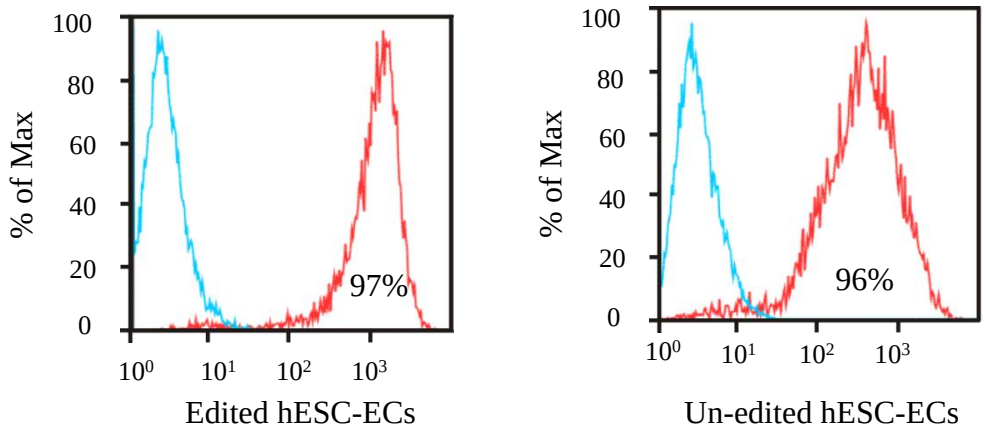

C

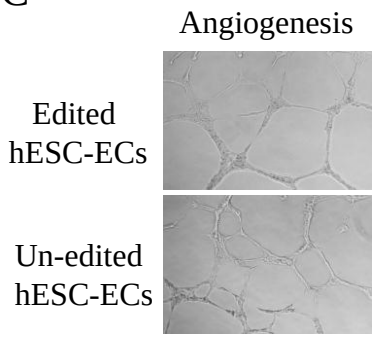

B

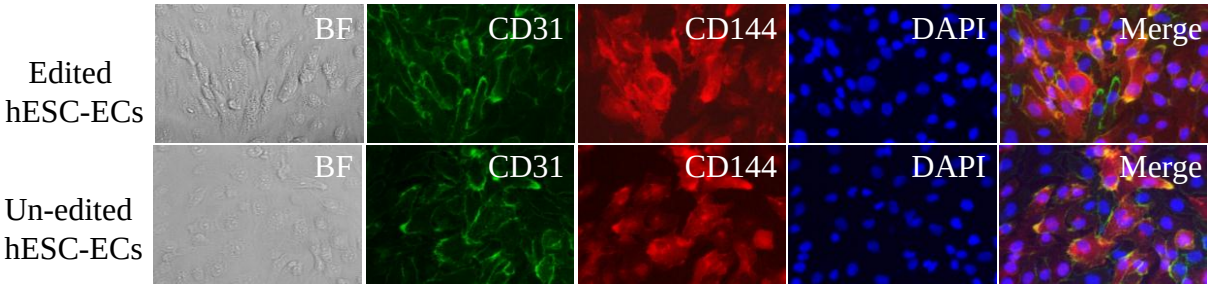

D

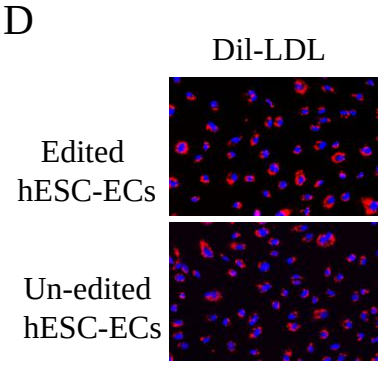

Online Figure VIII

SUPPLEMENTAL TABLE

Online Table I. Primers for detection of ZFN-editing and off target cleavage

Primers for ZFN integration detection	
AAVScaggs-1F	TATGGAGATCCCTCGACCTG
AAVScaggs-2F	CCAGCGGATCGACAGTACTAA
AAVS-1R	GTGAGTTTGCCAAGCAGTCA
AAVS-2R	GGTCCAGGCCAAGTAGGTG
Primers for off target site	
AAVS1Off-1F	TTTAAGAACTGTAACCTATTTTCCAAAGTGTTTG
AAVS1Off-1R	CCTGTAATCCCAGCTATTCGGGAG
AAVS1Off-2F	AAGGTGTAAGTGGAGCCACAAGGCT
AAVS1Off-2R	CAGGAAGAGCAGGAGATGAGGAGTT
AAVS1Off-3F	TTGGAAATAAGACCCATTTGTTGATGAGA
AAVS1Off-3R	CTGGCTCATTCCAACGTCCATGT
AAVS1Off-4F	GACTTGGTGGTTGGCAGAATACACC
AAVS1Off-4R	GGGTAAGGTCAGATAGGGCTGTAAGACTC
AAVS1Off-5F	GGAACAAGGCACCTGGCTCC
AAVS1Off-5R	CCATTCCCGGGAGAAATCTC
AAVS1Off-6F	TGAGTTTGGGCCTGAGGTCATC
AAVS1Off-6R	GGCTTGGAAACACCCAGGTG
AAVS1Off-7F	CTTTGAGTTTAGCAGCTTCCAGGAACC
AAVS1Off-7R	GTTTTATCTTCATAAGGTAGTGGGCAGATGG
AAVS1Off-8F	GGTCCTCACCCCATCTTCATC
AAVS1Off-8R	AAAGAGAGGGCTGGTGAGGC
AAVS1Off-9F	GGCTGTGACACTGTTGCAGGGAG
AAVS1Off-9R	CAGGCTCGTCCCATCCTTTTGC
Primers for AAVS1 target site	
AAVS1cut-F	TTCGGGTCACCTCTCACTCC
AAVS1_rev_Cel1	CTCAGGTTCTGGGAGAGGGTAG
AAVS1_fwd_Cel1	CCCCTTACCTCTCTAGTCTGTGC
AAVS1cut-R	GGCTCCATCGTAAGCAAACC

Online Table II. Off target sites *

Rank	Score	Chr	Location	Site	Gene
1	1.47E-09	8	141576215	GcTCCTGGCCCagTGCTGGCCACTGTGGGTGC	
2	8.39E-10	10	47105372	ACACCCACAGgGGCAGGGGcAGGGCCAGGAcT	
3	5.76E-10	4	3273229	TTTCCTGTCCtTtACCTGCCACTGTGGGTtT	
4	2.67E-10	10	117748684	TCACCCACAGatTTGTAATAGGGACAGGATT	
5	1.93E-10	9	137703230	GCACCCACAGcGcAGTGCcAGGGCCAGGAAC	
6	1.24E-10	14	100102870	GgTCCTGTCCCTgTGGGACCCACaGTGGGgGC	BEGAIN
7	1.13E-10	7	50638454	GTcCCTGTCCCTATATCCACACTGTGGcTGG	GRB10
8	9.84e-11	16	28904290	CATCCTGGCCaTgTTGATGgCACTGTGtGTGC	LAT
9	6.35e-11	12	48571253	CCACCCACAGgGcAGCCAGgAGGGACAGGATG	FAIM2

* These off target sites were identified by Hochemyer et al. [3]